



# Positron Emission Tomography

Physik Department TU München, Lehrstuhl E18  
<http://www.e18.physik.tu-muenchen.de/>

- Userguide for the lab course -

Location:

Nuklearmedizinische Klinik und Poliklinik der TU München  
Klinikum Rechts der Isar München  
Ismaninger Str. 22  
81675 München  
U4/U5, Max-Weber-Platz

<http://www.nuk.med.tu-muenchen.de/>

## 1. Abstract

**Introduction** Positron-Emission-Tomography or short PET is the state-of-the-art technique for imaging physiological processes inside humans or animals. This happens in a noninvasive fashion as the distribution of a radioactive, positron emitting radiopharmaceutical inside the body is monitored by surrounding detectors. With the help of mathematical algorithms, the tracer distribution is reconstructed to an image. PET has become an indispensable tool for ensuring the correct treatment of patients and assured diagnostics by the attending doctor, e.g. for cancer treatment. PET is heavily used in medicine, biology, neurology and pharmaceutical research as e.g. brain activity, blood flow or glucose flow can be monitored. Several interdisciplinary fields are merged within a running PET system, ranging from physics, communication technology, electrical engineering and image reconstruction up to the application in medicine. Thus there is a need for modern physicists to understand not only the underlying physics but also how the system works and is operated.

**Motivation** The one day laboratory course gives an introduction to PET, starting from the physical background up to the image reconstruction. An insight is given to detector techniques, modern readout electronics, data acquisition and analysis. Furthermore a short introduction to some standard tools in particle physics, e.g. Linux or the data analysis framework ROOT are part of this course. The PET scanner

## 1. Abstract

is a refurbished former small animal prototype, featuring 96 readout channels and set up with an up to date readout system. Data analysis and image reconstruction is done using a standard PC. The radioactive distributions which have to be reconstructed are different symbols milled in plexiglass, which are filled with a  $\beta^+$  decaying radionuclide. The available radioactive tracers are either  $^{18}\text{F}$  or  $^{22}\text{Na}$ .

**Guideline for Students** The userguide consists mainly of two parts: Before the lab course, it is essential to read and understand in every case the *Introduction* and the *Basics for the Image Reconstruction* part of the userguide ( $\rightarrow$ sec.2-4). The second part about *PET System Commissioning* and the *Tasks* ( $\rightarrow$ sec.5, 6) maybe cannot be fully understood without having the scanner in front of you, but is your guideline through the lab course. Nevertheless it must be read before. Most of the work is done during the lab course and you get the highest benefit for your knowledge, if you prepare yourself carefully. The evaluation should be the presentation of your results and must contain the answers to the questions given in your tasks ( $\rightarrow$ sec.6, p.40). It should be kept short. For taking your data with you, please bring a USB stick with a minimum capacity of 4 GB.

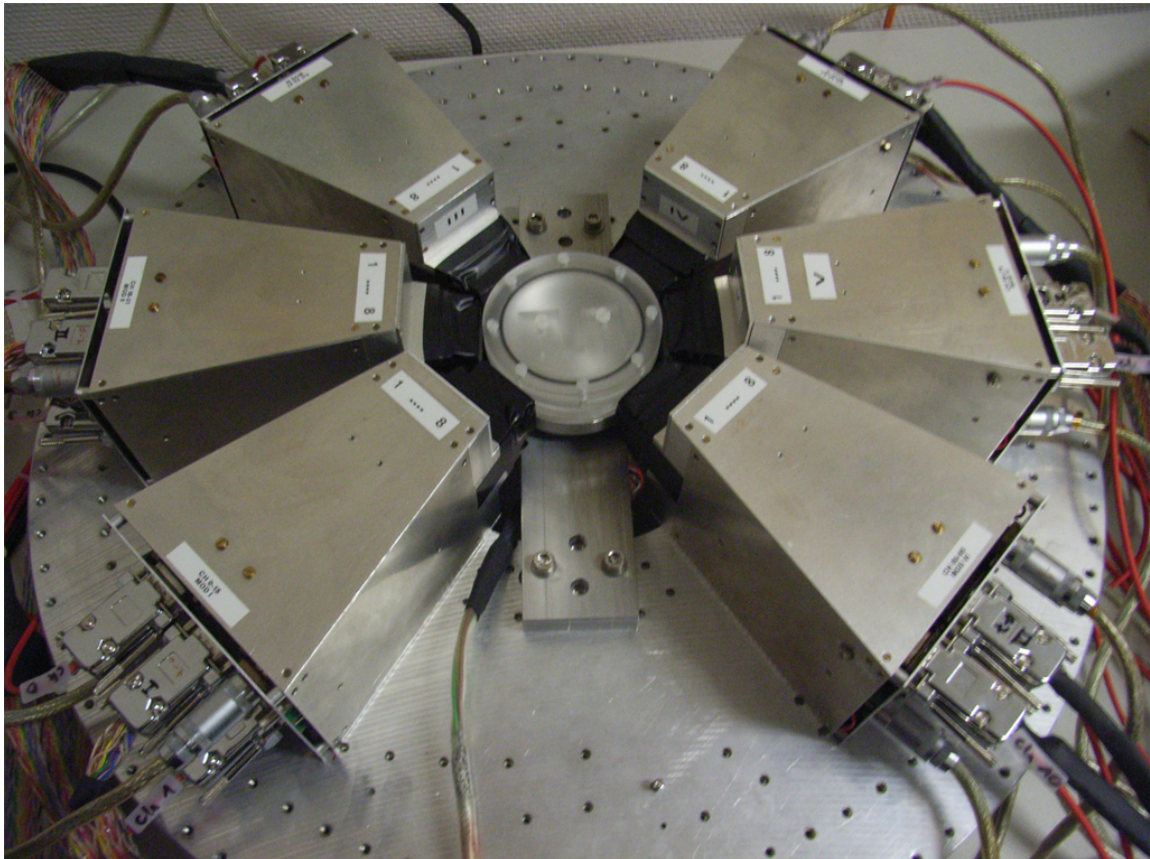


**Figure 1:** Image of the PET scanner for the lab course.

## 2. Introduction to Positron Emission Tomography

### 2.1. Positron Decay and Tracers

According to the Standard Model in particle physics, for every particle there exists an antiparticle. In case of the electron  $e^-$  with a charge of  $-1e$  and spin  $1/2$ , this is the positron  $e^+$  with a charge of  $+1e$ , spin  $1/2$  and the same rest mass of  $511 \text{ keV}/c^2$  as for the electron. Positrons can be created by either pair production or  $\beta^+$  decay.

**Pair Production** is the creation of an electron-positron pair from a photon interacting with the atomic nucleus. Therefore it is required that the photon provides enough energy for the process which is at least the total rest mass energy of  $1022 \text{ keV}/c^2$  of electron and positron together. This cannot happen in empty space since the nucleus is needed to conserve both energy and momentum. The quantum numbers are conserved since the photon has a total spin of 1 and zero charge.

$\beta^+$  **decay** is the basis for Positron Emission Tomography (PET), where instable and neutron poor nuclides achieve an energetic more favoured state by converting a proton to a neutron. To balance the charge, a positron  $e^+$  (also called  $\beta^+$  particle) is emitted:



The total energy release is shared between the daughter nucleus  ${}^A_{Z-1}\text{Y}$  and mainly both the positron with rest mass  $511 \text{ keV}/c^2$  and the electron-neutrino  $\nu_e$  with negligible small mass [KUC]. Thus positron emission shows an energy spectrum, as the kinetic energy is split between positron and neutrino, sometimes transferring almost the whole energy to one of them. The maximum energy transfer  $E_{\text{max}}$  is determined by the mass difference between parent and daughter nucleus, taking into account potential gamma-ray emission from excited states. The mean kinetic energy  $E_{\text{mean}}$  of the emitted positrons is about  $0.33 \cdot E_{\text{max}}$  ( $\rightarrow$ fig.2). Radionuclides which decay by positron emission can be used for PET imaging ( $\rightarrow$ tab.1). [PHE] [WUE] [KUC]

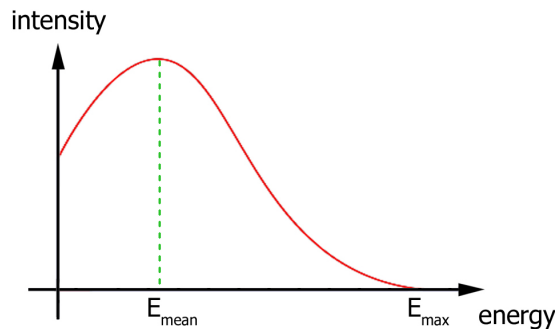


**Figure 2:** Energy spectrum for positrons emitted by  $\beta^+$  decay with their mean kinetic energy  $E_{\text{mean}} \approx 0.33 \cdot E_{\text{max}}$ .

## 2. Introduction to Positron Emission Tomography

| Radionuclide     | Half-life | $E_{\max}$ (MeV) | $\beta^+$ Branching ratio |
|------------------|-----------|------------------|---------------------------|
| $^{11}\text{C}$  | 20.4 min  | 0.96             | 1.0                       |
| $^{13}\text{N}$  | 9.97 min  | 1.20             | 1.0                       |
| $^{15}\text{O}$  | 122 s     | 1.73             | 1.0                       |
| $^{18}\text{F}$  | 109.8 min | 0.63             | 0.97                      |
| $^{22}\text{Na}$ | 2.60 y    | 0.55             | 0.90                      |

**Table 1:** Radionuclides which decay by positron emission. Most widely used for PET are  $^{11}\text{C}$ ,  $^{13}\text{N}$ ,  $^{15}\text{O}$  and  $^{18}\text{F}$ . The branching ratio gives the fraction of particles undergoing a  $\beta^+$  decay with respect to the total number of particles decaying. [PHE] [MAN]

Most widely used are  $^{11}\text{C}$  (cardiology, oncology),  $^{13}\text{N}$  (cardiology),  $^{15}\text{O}$  (cardiology, neurology) and  $^{18}\text{F}$  (cardiology, neurology, oncology). Since the radionuclides behave chemically like their corresponding stable isotopes, the process of chemical synthesis is identical for radioactive and non-radioactive substances. This offers the possibility to place such a radioactive molecule into a dynamical system, where it is used as a tracer by monitoring its distribution from the outside with the help of detectors. This is done for PET, where e.g. the tracer is radioactive labelled glucose. The glucose ( $\text{C}_6\text{H}_{12}\text{O}_6$ ) molecules itself are labeled by replacing an  $\text{OH}^-$  group with the  $\beta^+$  decaying  $^{18}\text{F}$ , resulting in fluorodeoxyglucose or short **FDG** ( $\rightarrow$ fig.3).

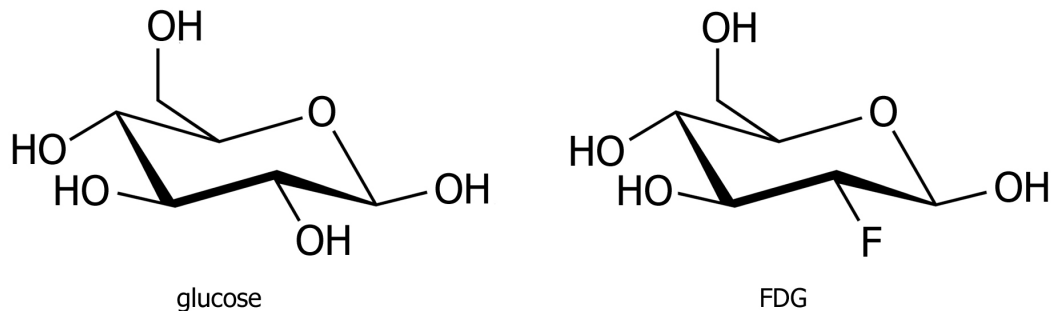


**Figure 3:** Glucose and FDG molecule, where one  $\text{OH}^-$  group is substituted by  $^{18}\text{F}$

After injecting FDG into a patient's body it behaves the same way as any non-radioactive glucose molecule. This allows to make the glucose metabolism visible. As e.g. cancer tissue shows a higher glucose consumption than surrounding tissue, more activity is accumulated there. A PET system is able to detect and image the activity distribution. In the final image it is then possible to identify the regions affected by cancer ( $\rightarrow$ fig.4). The same principle applies to the monitoring of brain activities with a higher glucose uptake of stressed regions ( $\rightarrow$ fig.5).

Due to the short half life of the mentioned radionuclides, they have to be produced just in time before their use. Only  $^{18}\text{F}$  can be stored for some hours and is beside  $^{22}\text{Na}$  most suitable for developing a detector system or the use in a laboratory course.  $^{22}\text{Na}$  is used in form of common salt  $\text{NaCl}$ , where the stable sodium has been replaced

by the radioactive isotope.

The production of the tracer is done with a particle accelerator, e.g. a cyclotron, that accelerates hydrogen ions ( ${}^1_1\text{H}^+$ ), deuterium ions ( ${}^2_1\text{H}^+$ ) or  $\alpha$  particles ( ${}^4_2\text{He}^{2+}$ ) to energies of about 8 - 15 MeV which then are shot on a production target. There, nuclear reactions ((p,n), (d,n), (d, $\alpha$ ), ( $\alpha$ ,n)) produce the tracer isotope. Through radiochemical processes first the tracers are removed from the target material and then the radiopharmaceuticals are synthesized. Because of the high costs of the whole production process only a few sites can afford to operate both a cyclotron and a PET scanner close to each other.

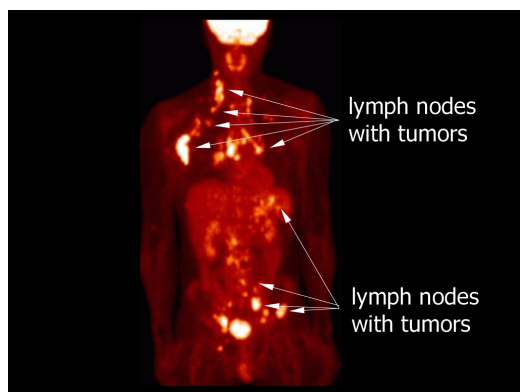


**Figure 4:** PET image of a cancer patient.  
[BOE]

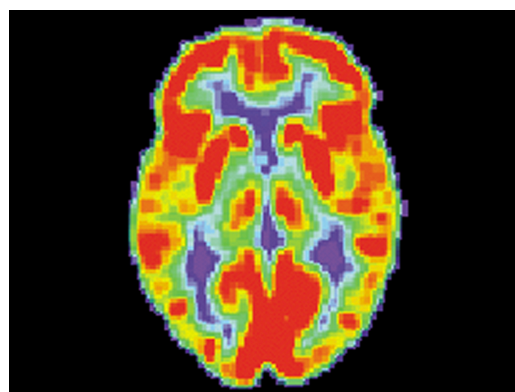


**Figure 5:** Healthy brain image taken with a PET scanner.  
image source:  
<http://commons.wikimedia.org>

As a summary, PET allows to make metabolisms visible, using different tracers for monitoring the desired biochemical process. FDG nowadays is the most widely used radiotracer for PET due to its advantageous half life. The more short-lived tracer nuclides like  ${}^{15}\text{O}$  and  ${}^{13}\text{N}$  are mainly used for monitoring of blood flow properties and to distinguish between vital and necrotic tissue in cardiology and neurology. [MAN]

## 2.2. Positrons in Matter and Annihilation

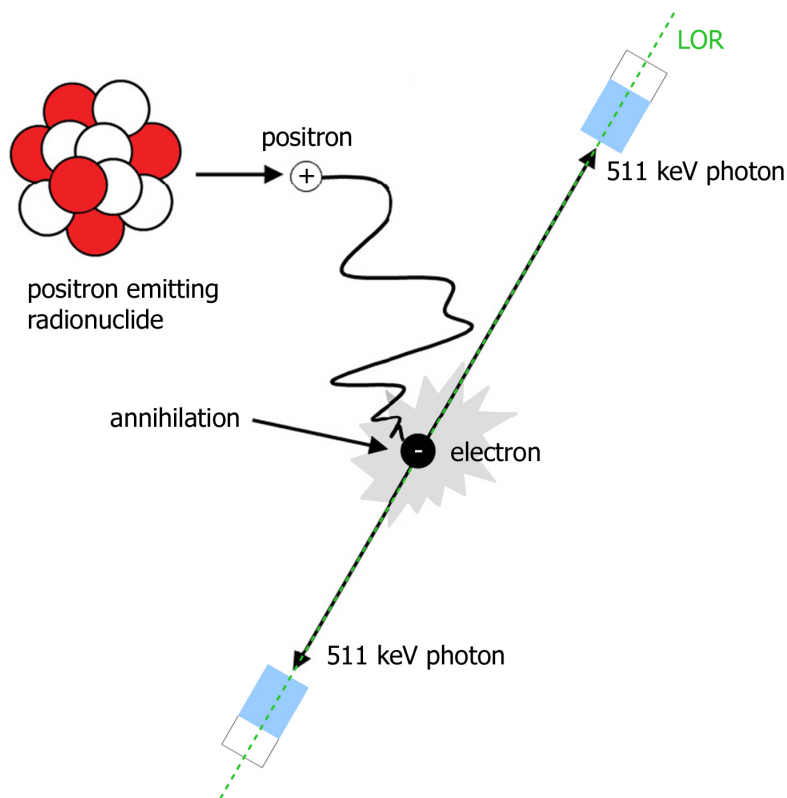


**Figure 6:** Annihilation of positron and electron, resulting in two 511 keV photons 180° apart, detected by two opposing detectors. The points of detection can be joined by a line, on which the annihilation must have taken place. The site of annihilation is usually very close to the point of  $\beta^+$  decay, as positrons rapidly lose their energy in material or tissue.

In matter, positrons are affected by the Coulomb force because of their electric charge. A positron released by  $\beta^+$  decay thus collides inelastically with the atomic electrons in the surrounding material, losing rapidly its kinetic energy. The range is typically about 0.1 to 1 mm, depending on the initial energy. Almost at rest, the positron combines with an electron to form a hydrogen-like state called positronium - in analogy to hydrogen, but the proton is substituted by the positron. The lifetime is only about  $10^{-10}$  s before  $e^-$  and  $e^+$  annihilate, where the mass of electron and positron is converted into at least two photons. Because both  $e^-$  and  $e^+$  now have negligible kinetic energy compared to their masses, the energy release is mainly from the particle mass and using Einstein's mass energy equivalence (with  $c = 2.998 \cdot 10^8 \frac{\text{m}}{\text{s}}$  the speed of light,  $e^-$  and  $e^+$  masses  $m_{e^-} = m_{e^+} = 511 \frac{\text{keV}}{c^2}$ )

$$E = mc^2 = m_{e^-}c^2 + m_{e^+}c^2 \quad (2)$$

the energy release is 1022 keV. [PHE]

As the positron and electron are almost at rest when annihilation occurs, the net momentum is almost zero. Because of energy and momentum conservation, annihilation to a single photon is generally not possible - otherwise a net momentum would occur in the direction of that photon. Most probable is the creation of two photons, which are emitted simultaneously in opposite directions due to momentum conservation,  $180^\circ$  apart. The total energy of 1022 keV is split equally to both resulting in  $511 \text{ keV}/c^2$  per photon.

These facts are the key for PET. On one hand, the annihilation photons are ten times

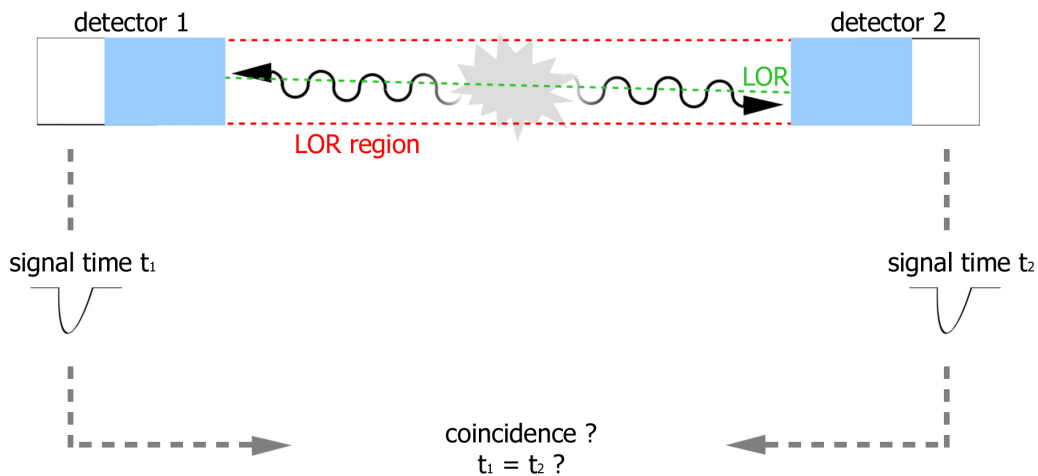


**Figure 7:** Coincidence of the detected photons is crucial for a valid LOR. The width of the LOR region is defined by the size of the active area of the opposing detectors.

more energetic than diagnostic x-rays, which leads to a very good chance to escape e.g. the patient's body for external detection. On the other hand, the characteristic and precise geometric release of the photons provides the spatial information, where the annihilation happened. The site of decay and annihilation are typically within distances from 1 - 0.1 mm in tissue, depending on the positron's initial energy [PHE]. Since this is very close, the annihilation directly correlates to the location of the radionuclide. Joining the points of detection results in the so called line of response **LOR** ( $\rightarrow$ fig.6), which is the basis for image reconstruction. Somewhere on this line the annihilation took place. Additionally it is necessary to have the time information for every detected photon to ensure, that both photons originate from the same annihilation and thus hit the detectors in coincidence. This is crucial for a correct assignment of a LOR ( $\rightarrow$ fig.7) as usually many photons in short times are detected. For real detectors, a region for valid LORs between two detectors is defined by the size of their active area. Only events from simultaneously detected photons in opposing detector pairs are the desired ones for PET imaging. The tracer activity correlates directly to the number of created annihilation photons, as generally for every  $\beta^+$  decay one annihilation takes place.

### 2.3. Photons in Matter

After annihilation, the photons travel in the surrounding material like e.g. tissue or the detector material. For 511 keV annihilation photons, the dominating interaction mechanisms are the photoelectric effect and Compton scattering. Pair production, where an electron-positron pair is created from an high energetic photon, is not possible, as the photon must have at least an energy of 1022 keV equivalent to the masses of  $e^+$  and  $e^-$  together. Therefore it is not mentioned in the following.

#### Photoelectric Effect

An incoming photon transfers all its electromagnetic energy  $E_\gamma$  to an atomic electron

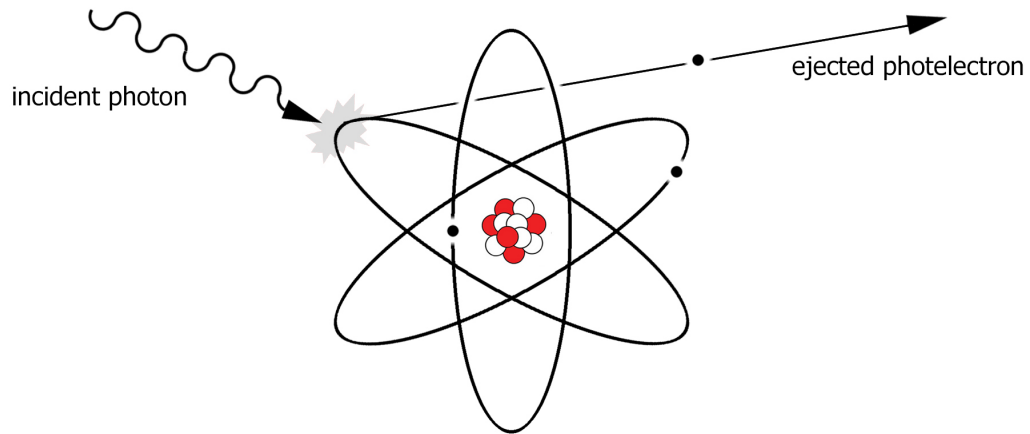


**Figure 8:** Schematic of photoelectric effect. The incident photon transfers all its energy to an atomic electron and ejects it from the atom.

and is absorbed ( $\rightarrow$ fig.8). The electron's kinetic energy now is sufficient to escape the atom, leaving a vacancy, which is filled again with another electron from the proximity. This process generates x-rays with a typical energy of tens of keV corresponding to the binding energy of the kicked out electron. In reasonably dense solids or liquids a photoelectric interaction deposits the complete energy of the absorbed photon locally within a sphere of a few hundred microns in diameter [PHE]. The photoelectric effect is roughly proportional to  $1/E_\gamma^{-7/2}$  and  $Z^5$  with  $Z$  the atomic number of the absorbing material. [DE4]

#### Compton Scattering

Figure 9 shows a Compton scattering interaction. Here the incident photon scatters off a free or loosely bound electron of the medium, transferring only some of its energy. Thus the photon is not absorbed, but changes its direction. Since energy and momentum have to be conserved, this leads to the energy of the scattered photon

$$E_{sc} = \frac{m_e c^2}{\frac{m_e c^2}{E_\gamma} + 1 - \cos \theta} < E_\gamma \quad (3)$$

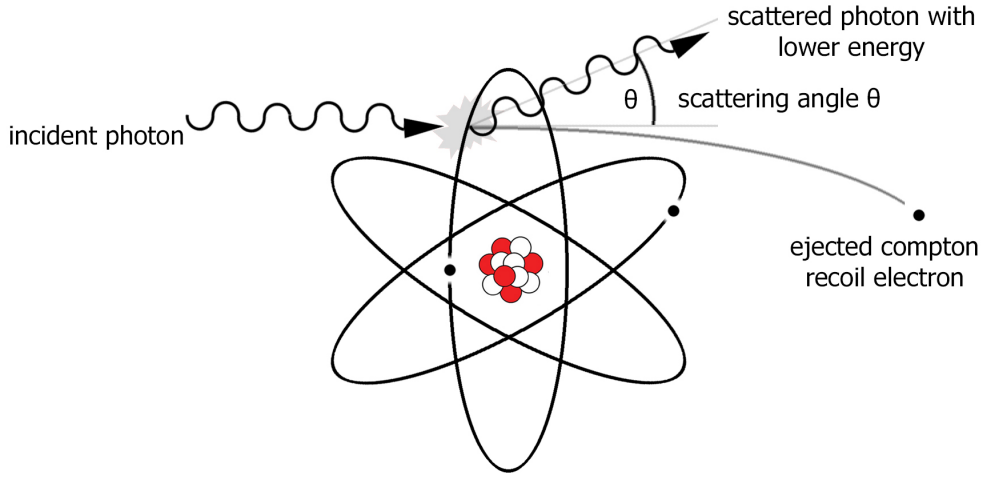


**Figure 9:** Schematic of Compton scattering. The incident photon transfers a part of its energy to an atomic electron and is deflected.

with  $E_\gamma$  the energy of the incoming photon,  $E_{sc}$  the energy of the scattered photon,  $\theta$  the scattering angle, the electron mass  $m_e$  and  $c$  the speed of light. For PET with 511 keV photons this simplifies to

$$E_{sc}[\text{keV}] = \frac{511}{2 - \cos \theta} \quad (4)$$

The recoil energy  $E_{rc} = E_\gamma - E_{sc}$  which is transferred to the electron dissipates inside the medium. The maximum energy loss occurs when the 511 keV photon is scattered by  $\theta = 180^\circ$ . This results in  $E_{sc} = 170$  keV for the remaining photon energy and  $E_{rc} = 341$  keV for the recoil energy given to the electron. The scattered photons are visible in the energy spectrum. For PET this is important as usually photons with an energy deposit of less than 480 keV are not taken into account during the search for LORs ( $\rightarrow$ sec.5.6, p.35). The Compton effect is roughly proportional to  $1/E_\gamma$  and  $Z$ . [PHE] [DE4]

## 2.4. Photon Detection and PET System Requirements

### 2.4.1. Scintillators

Scintillators are transparent organic or anorganic liquids or solids that are luminescent. When hit by a particle or high energy photon, they absorb its energy and scintillate, i.e. emit the absorbed energy in form of light in the visible range.

The scintillator material of choice for our detectors is LSO due to its high light yield and fast decay time compared to other common scintillators for PET ( $\rightarrow$ tab.2).

| Scintillator                       | Density (g/ccm) | Light output (photons per 511 keV) | Decay time (ns) | Index of refraction | Linear attenuation at 511 keV (cm <sup>-1</sup> ) | Ratio between photoelectric and Compton |
|------------------------------------|-----------------|------------------------------------|-----------------|---------------------|---|---|
| Bismuth Germanate (BGO)            | 7.13            | 4200                               | 300             | 2.15                | 0.96  | 0.78                                    |
| Lutetium Oxyorthosilicate (LSO:Ce) | 7.40            | ~13000                             | ~47             | 1.82                | 0.88  | 0.52                                    |
| Barium Fluoride (BaF2)             | 4.89            | 700, 4900                          | 0.6, 630        | 1.56                | 0.45  | 0.24                                    |

**Table 2:** Properties of different scintillator materials. [KNO]

### 2.4.2. Photodiodes

#### Semiconductor Doping

The basis for photodiodes is the doping of semiconductors. Doping is the process of building crystal impurities into a pure semiconductor to change its electrical properties (→fig.10). The pure semiconductor used is silicon Si. Each Si atom is bound covalently by its 4 binding electrons to another Si atom in the crystal. By doping the crystal with e.g. B (boron, 3 binding electrons), per added B atom there is one electron less available for the covalent binding. This creates a net positive charge also called *hole*. Such doped crystals are known as p-doped. On the other hand, replacing a Si atom with e.g. P (phosphorus, 5 binding electrons) results in an additional electron inside the crystal, now being n-doped. Nevertheless the crystal as a whole still appears electrical neutral to the outside, but with changed properties in charge transport.

#### Silicon Photodiodes

Silicon photodiodes consist of two thin layers of p and n doped silicon with electrodes on top and bottom (→fig.11). The p-n junction allows electrons from the n-doped region to diffuse into the p-doped region. There they can fill the positive 'holes'. The result is an electric field in the border region which is positive on the n side (less electrons than before) and negative on the p side (less holes and more electrons than before). The region between the junction now has no more free charge carriers due to the recombination of electrons and holes and is therefore called *depletion zone*. This

## 2.4. Photon Detection and PET System Requirements

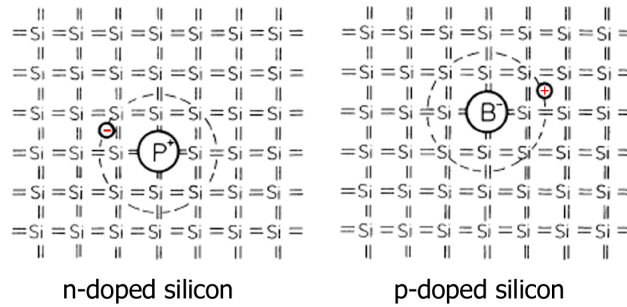


**Figure 10:** Illustration of silicon doping with boron and phosphorus.

image taken from the userguide of the lab course in photovoltaics offered at TUM physics department:  
<http://www.physik.tu-muenchen.de/studium/betrieb/praktika/fopra/text/userguide-50.de.pdf>

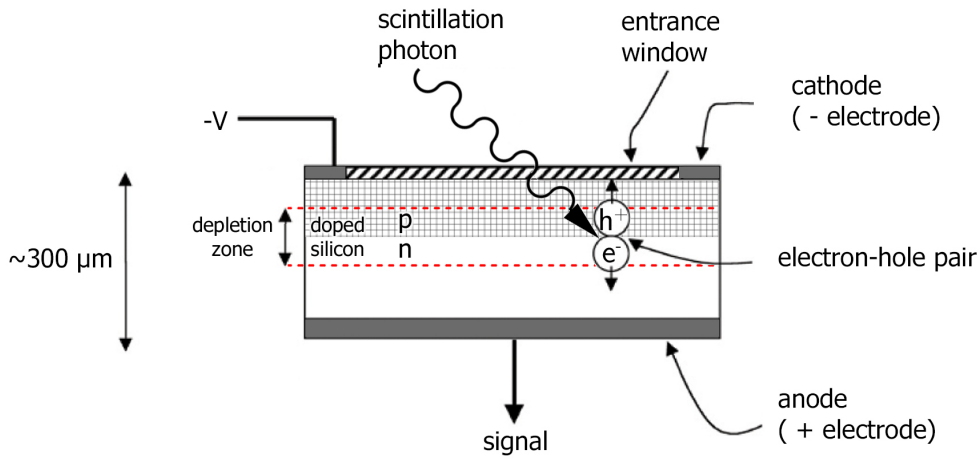


**Figure 11:** Scheme of a photodiode.

zone grows due to recombination, which results finally in a steady state as electrons are no longer able to pass the depletion zone.

If an incoming photon is absorbed in or very close to the depletion zone, it frees an electron leaving a hole. This electron-hole pair feels the electric field of the p-n junction and so the electron drifts towards the anode (positive electrode) and the hole towards the cathode (negative electrode). If anode and cathode are shortened, this produces a measurable photocurrent between them. Otherwise a voltage builds up. The quantum efficiency of photodiodes is approximately 60% to 80%.

The width of the depletion zone can be modified by applying a voltage across the photodiode. To decrease the width, the p material is connected to the positive terminal and the n material to the negative terminal. This state of operation is called *forward bias* and usually makes the photodiode conduct, as the holes as well as the electrons are forced towards the junction and recombine there. To increase the depletion zone and its electric field strength, the n material is connected to the positive terminal and p to the negative terminal, called *reverse bias*. This pulls the holes in p away from the junction, the same is true for the electrons in the n material.

## 2. Introduction to Positron Emission Tomography

It increases the voltage barrier and causes a high resistance.

### **APD - Avalanche Photodiodes**

As standard photodiodes have no internal gain, they produce just one electron-hole pair per photon interaction. Thus their signal is about  $10^6$  times weaker than that of a PMT due to the missing amplification, which makes them unsuitable for PET. To solve this, the standard photodiode is modified by applying a higher voltage across the photodiode (reverse bias) and a different doping structure. An incoming photon now causes the diode to breakdown. This breakdown process is non-destructive and reversible, so long as the amount of current flowing does not reach levels that cause the semiconductor material to overheat and cause thermal damage. The field strength of the depletion zone is now that high, that the created electrons gain enough kinetic energy to free further electrons on their way to the anode. Due to this electron avalanche, the diode is now called avalanche photodiode (APD) and has a typical gain of  $10^2$  to  $10^3$ . [PHE]

To compensate the still lower gain versus a PMT, scintillators with a high light yield are deserved to get a higher initial signal. APDs are roughly equivalent in energy and time performance compared with PMT-based detectors, but allow a more compact detector assembly and are able to operate in high magnetic fields up to 9.4 Tesla [PIC], which makes them suitable to combine PET and MRT. Disadvantage of APDs is their strong temperature dependence, which requires regular detector calibration and operation in steady environmental conditions.

### 3. Basics for the Image Reconstruction

The goal of image reconstruction is to provide a crosssectional 2D view of the  $\beta^+$  distribution of the decaying atoms inside the scanned object.

#### 3.1. Theoretical Background

This section gives you the theoretical fundament for the image reconstruction done in the lab course. For an easier entry, let us assume a simplified PET scanner in the following. It consists of a single ring of individual photon detectors ( $\rightarrow$ fig.12).

##### 3.1.1. Sinogram

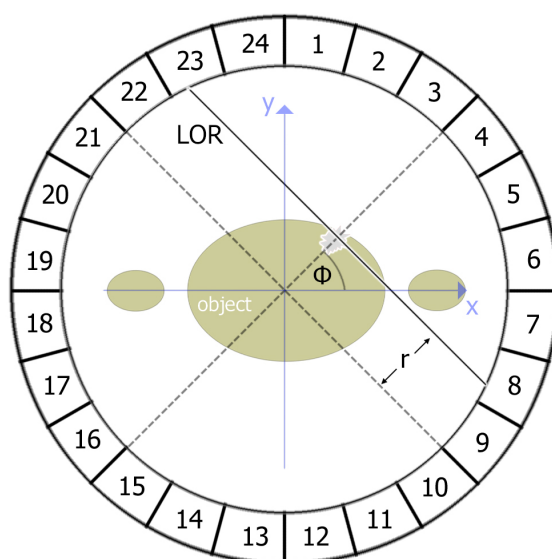


**Figure 12:** Simple PET scanner ring with 24 detectors. This shows the way, how LORs are stored into sinograms. The origin of both  $(x, y)$  and  $(r, \phi)$  coordinate systems is the center of the field of view.

A sinogram is a 2-D matrix into which all found coincidences from a pet scan are histogrammed. It is the basis for the application of the mathematical reconstruction algorithms. Each element in the matrix corresponds to the number of valid LORs which have been recorded by a certain pair of opposing detectors.

In our example ring scanner shown in figure 12, only directly opposing detector pairs are allowed to have coincidences with each other, resulting in a  $12 \times 12$  matrix ( $\rightarrow$ fig. 13). By allowing one detector not only to have coincidences with its direct opponent but also with neighbouring opposing ones, the number of matrix elements increases accordingly. In the matrix, LORs with equal angles  $\phi$  are in the same row and the columns stand for equal radial distances  $r$  with respect to the center of the field of view. The shown example LOR between detectors 23 and 8 results in

### 3. Basics for the Image Reconstruction

a sinogram matrix entry corresponding to the LOR's  $\phi$  and  $r$ . It is quite obvious that the non-infinitesimal small size of the detector's active area results in a certain tolerance for the LOR angle  $\phi$  and the radial distance  $r$  ( $\rightarrow$ fig.7, p.7).

The mathematical relationship between the  $(x, y)$  detector coordinate system and the LOR coordinate system  $(r, \phi)$  is given by

$$r = x \cdot \cos\phi + y \cdot \sin\phi \quad (5)$$

Both detector and LOR coordinate system have their origin in the centre of the field of view.

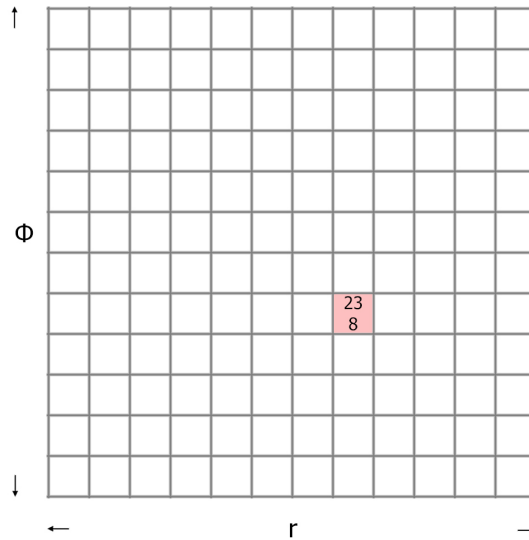


**Figure 13:** Sinogram matrix. Detector pairs in rows are equal in angle  $\phi$ , the ones in columns are equal in  $r$ . As an example, the LOR from figure 12 adds one entry to the matrix element that stands for detectors 23 and 8.

The name sinogram arises from the fact, that the LORs of a point source arranged in the matrix draw a sinusoidal path. An example of a phantom with two point sources and its corresponding sinogram is shown in figures 14 and 15.

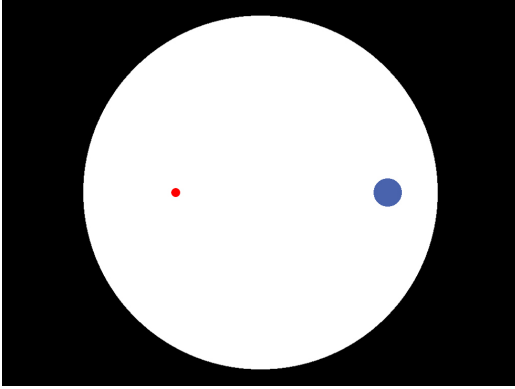


**Figure 14:** A phantom with two point sources.

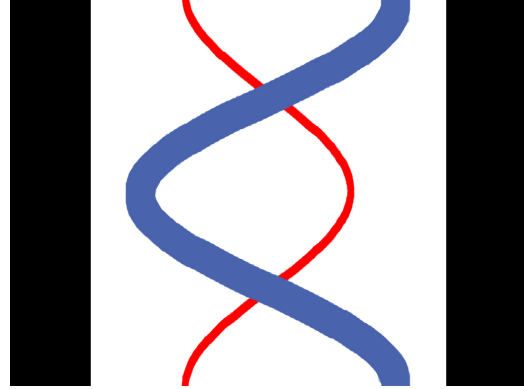


**Figure 15:** Illustration of the sinogram for the two point sources from figure 14 for a  $360^\circ$  pet scan. Each point source draws a sinusoidal path.

### 3.1.2. Backprojection BP

The most basic reconstruction method is the linear superposition of all LORs, where the field of view is pixelized. For a valid LOR, a line is drawn through the pixels ( $\rightarrow$ fig. 16). The value added to each pixel is given by  $M \cdot w$  with  $M$  the number of alike LORs in this pixel and  $w$  the weighting factor that depends on the pathlength of the LORs inside the pixel. In other words, the registered annihilation photons from a detector pair are being projected back along the line from which they originated. This is repeated for all valid LORs and finally a weighting image of LORs is produced. Figure 16 also shows the limits of this method: many points where no decay happened contribute to the final image, resulting in a typical blurring at the borders of the activity. Mathematically, the backprojected image  $b(x, y)$  results from a convolution of the true activity distribution  $a(x, y)$  with the typical  $1/r$  decline for backprojection

$$b(x, y) = a(x, y) * \frac{1}{r} \quad (6)$$

where  $r$  is the distance to the real activity border. So backprojection is only an approximation method and generally not suitable for more complex activity distributions.

Data processing with a computer allows two different approaches to backprojection. The above mentioned is known as *ray-driven backprojection*, the other more common and efficient way is to perform backprojection out of stored sinogram data ( $\rightarrow$  sec.3.1.1) known as *pixel-driven backprojection*, which is also used for this project. Here for each image pixel  $(x, y)$  and each projection angle  $\phi$ , one calculates the sinogram coordinate  $r$  ( $\rightarrow$  eq.5) that contributes to that pixel. All pixels are handled consecutively and all possible projection angles are taken into account before pro-

### 3. Basics for the Image Reconstruction

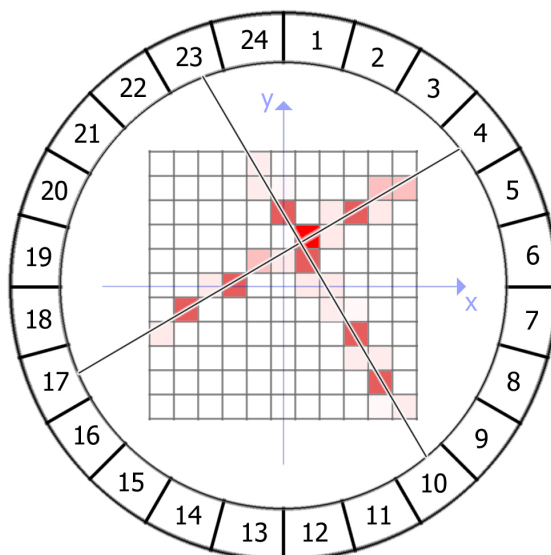


**Figure 16:** Schematic of simple backprojection with LORs between detectors 4/17 and 10/23. The field of view is pixelized and each pixel weighted depending on how long the pathlength of the LOR inside a pixel is.

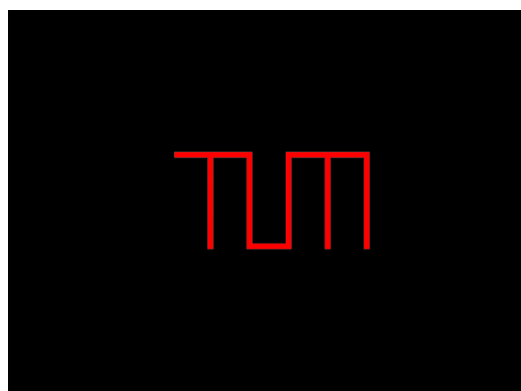


**Figure 17:** Phantom source with TUM logo that shows the exact activity distribution.

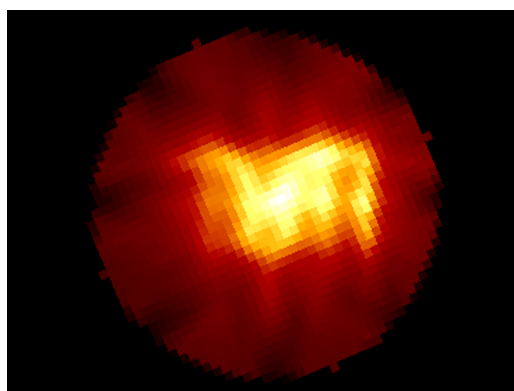


**Figure 18:** Measurement with an activity of 0.7 Mbq and FDG. Reconstruction of the TUM logo using simple backprojection and sinogram data. The  $1/r$  blurring is noticeable.

cessing the next pixel. Hence the backprojected image  $b(x, y)$  can be described by

$$b(x, y) = \frac{1}{N} \sum_{n=1}^N s(r, \phi_n) = \frac{1}{N} \sum_{n=1}^N s(x \cdot \cos \phi_n + y \cdot \sin \phi_n, \phi_n) \quad (7)$$

with  $N$  the number of different equally spaced projection angles over which data has been obtained.  $s(r, \phi_n)$  stands for the number of counts in the sinogram element at

angle  $\phi_n$  and the radial distance  $r$ . [PHE]

### 3.1.3. Filtered Backprojection FBP

#### Fourier Transform

The mathematical prerequisite for enhancing the image quality of simple BP is the Fourier transform. It transforms a function  $f(x)$  in terms of its component spatial frequencies  $\nu$  as a sum of weighted sine and cosine terms.

$$F(\nu) = FT[f(x)] = \int_{-\infty}^{\infty} f(x)e^{-2\pi i\nu x} dx = \int_{-\infty}^{\infty} f(x)(\cos(-2\pi\nu x) + i \sin(-2\pi\nu x)) dx \quad (8)$$

The frequencies  $\nu$  and the magnitude of the frequencies  $F(\nu)$  are determined by how much the function  $f(x)$  changes with position. E.g., a function  $f(x)$  that is fairly uniform is represented by lower frequencies while another one with rapid changes and sharp discontinuities requires higher frequencies for an appropriate determination.

The inverse Fourier transform to get back the original function is given by

$$f(x) = FT^{-1}[F(\nu)] = \frac{1}{2\pi} \int_{-\infty}^{\infty} F(\nu)e^{2\pi i\nu x} d\nu \quad (9)$$

#### Filtered Backprojection

FBP is able to compensate the  $1/r$  blurring that occurs with simple BP. For this, it is necessary to apply a filter on the frequency behaviour of the original projection data  $s(r, \phi)$ . The goal is not to lose information about the location of the activity but to get rid only of the blurring. One exploits, that in the frequency domain of  $s(r, \phi)$  higher frequencies correspond to locations with higher activity and vice versa. For a certain projection angle  $\phi_n$  (rows in the sinogram matrix), a 1-D Fourier transformation is enough as one only wants to filter the  $r$  dependency of the sinogram data. It gets

$$S(\nu) = FT[s(r, \phi_n)] = \int_{-\infty}^{\infty} s(r, \phi_n)e^{-2\pi i\nu r} dr \quad (10)$$

and applying the filter function  $C(\nu)$  the backtransform reads

$$s_*(r, \phi_n) = FT^{-1}[C(\nu) \cdot S(r, \phi_n)] \quad (11)$$

where  $s_*(r, \phi_n)$  is now the filtered sinogram data. This is repeated for every matrix element of the sinogram and the new corrected matrix is processed the same way as done for the simple backprojection. Hence, the name filtered backprojection.

Usually, the filter  $C(\nu)$  is a ramp filter that favors higher frequencies ( $\rightarrow$ fig.19), which gives 'sharpness' to the reconstructed image and additionally can be modified to improve the signal to noise ratio.

The cutoff frequency  $\nu_{\max}$  is given by

$$\nu_{\max} = \frac{1}{2 \cdot \Delta r} \quad (12)$$

### 3. Basics for the Image Reconstruction

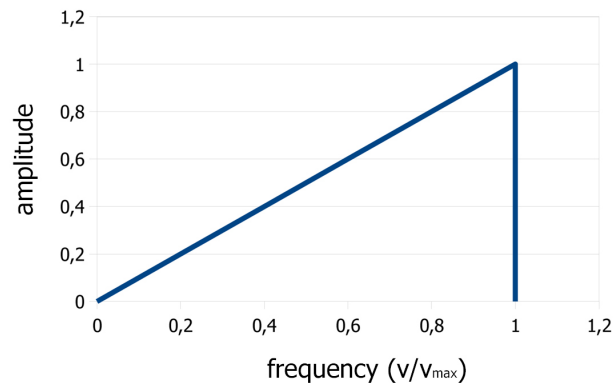


**Figure 19:** Filter ramp function with a cutoff at the frequency  $\nu_{\max}$ .

with  $\Delta r$  the distance between two samples in the sinogram. It results from the limited sampling accuracy of the detector system, as each detector has a non-infinitesimal small active area.

## 4. PET System and Components

This section gives an overview of our PET system and concentrates the most important specifications of the hardware. Figure 20 shows a picture of the complete system. The main parts are the detector ring, the powercrate and the readout PC.

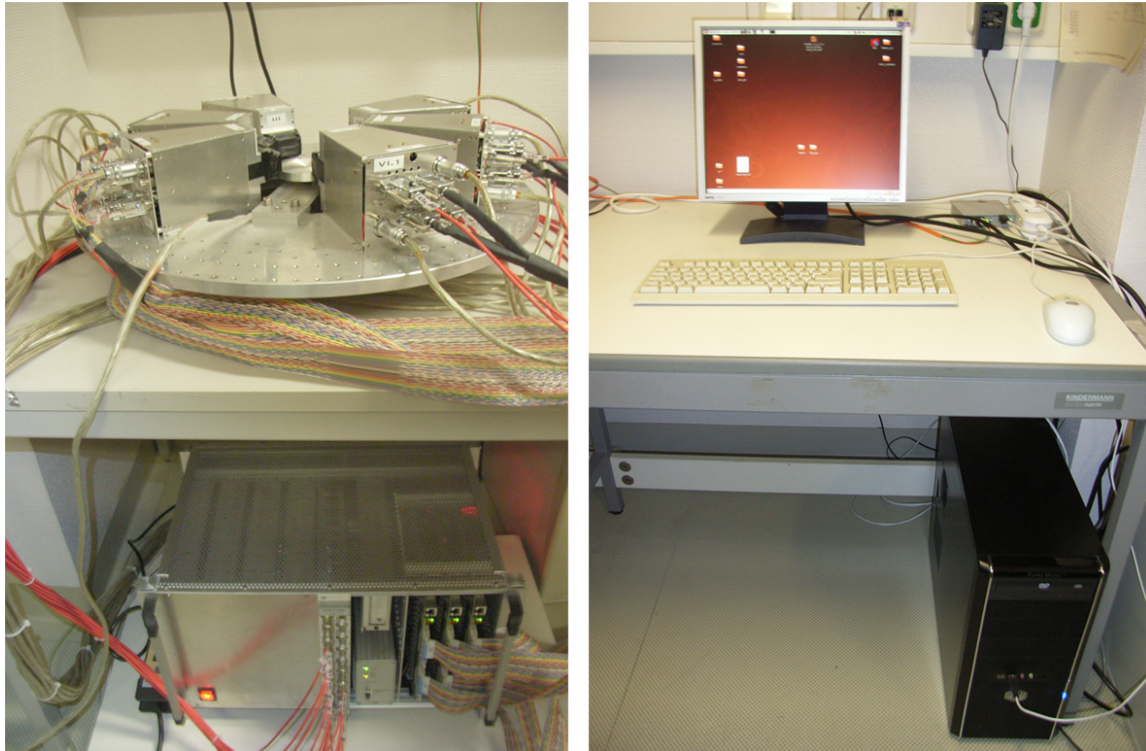


**Figure 20:** Overview of the complete PET system as used in the lab course.  
*Left:* On the table is the PET scanner, under the table stands the powercrate.  
*Right:* Readout workstation with Linux PC.

## 4. PET System and Components

### 4.1. Detector System

The detector system was a former prototype scanner for small animal PET. Due to the use of APDs as scintillation light detectors, it was called *Munich Avalanche Diode Positron Emission Tomograph* or short MADPET. It provides a field of view (FOV) diameter of 86 mm. To get a better overview of the data flow, a schematic of

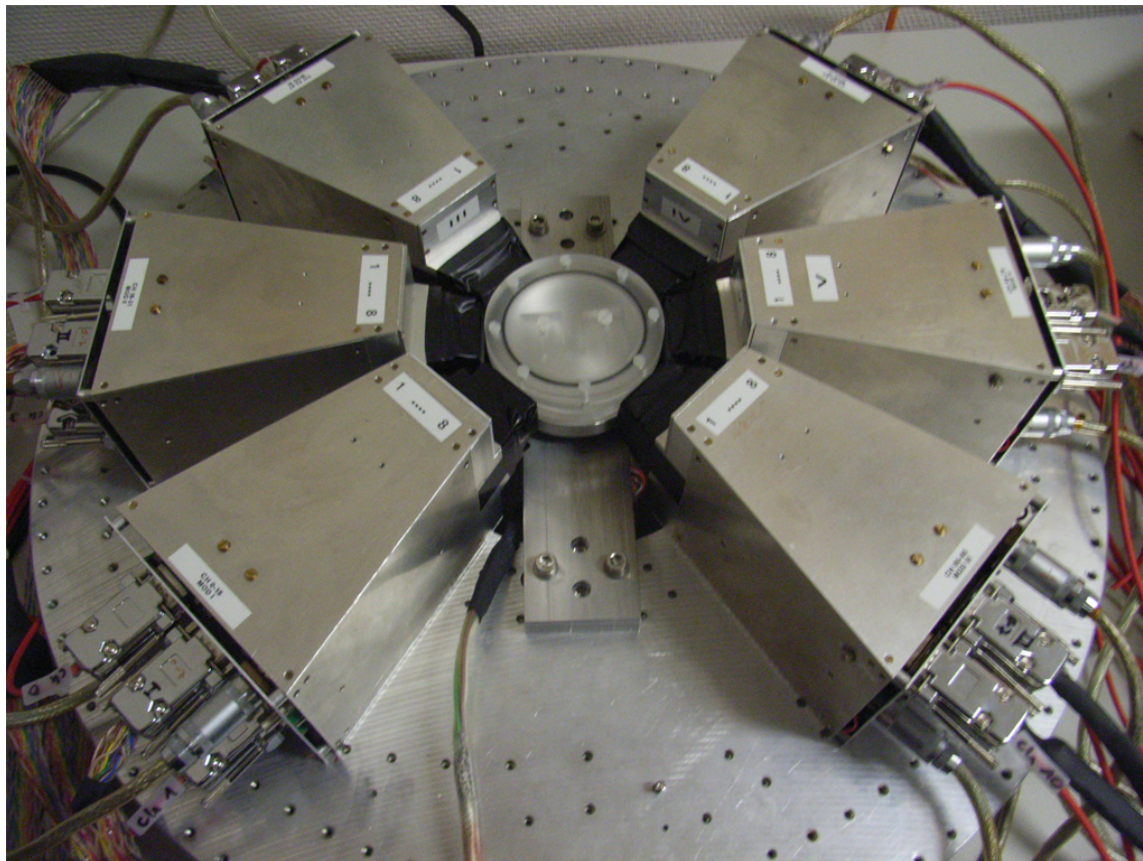


**Figure 21:** MADPET sector tomograph in the current configuration for the lab course with in total 6 detector modules: each has two rows of APDs with 8 channels per row, resulting in 96 channels in total. The modules are arranged at the borders of a octagon. In the center, a radioactive source is placed, which is rotated during the scan process to cover all projection angles.

the readout system is illustrated in figure 22. The signals from in total 96 individual and independent detector channels are processed with 3 modern SADCs (sampling analog to digital converter). They digitize the analogous detector signals and do a time and amplitude extraction. Each of them can handle 32 channels. Every SADC is equipped with one J2-USB card with a single USB port for data readout, resulting in 3 USB cables connecting the frontend electronics to a standard PC running Linux. One of the J2-USB cards also activates the stepping motor, since the system runs as sectorized tomograph and it is therefore necessary to rotate the radioactive sources to cover all projection angles. The PC is responsible for data aquisition and processing,

the stepping motor control and finally the image reconstruction.

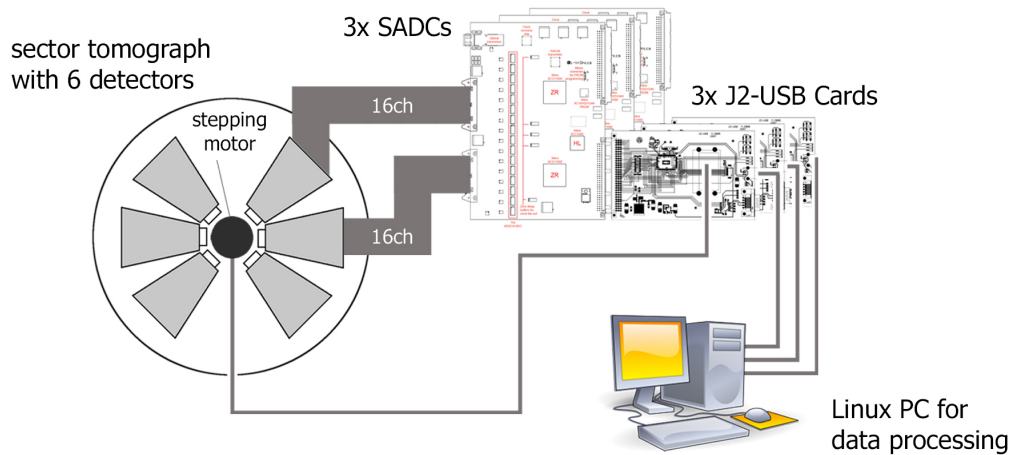


**Figure 22:** Schematic of the used readout system. Each detector module features 16 channels, two of them are connected to one SADC. For a total of 96 detector channels, 3 SADCs are needed, each equipped with a J2-USB card. One of these cards is also able to activate the stepping motor.

#### 4.1.1. Scintillators, APDs and Detector Modules

A single detector channel consists of one LSO scintillator crystal with the dimensions of  $3.7 \times 3.7 \times 12.0 \text{ mm}^3$ , coupled to one APD with an active area of  $4 \times 4 \text{ mm}^2$ . 16 single APDs are placed in a  $2 \times 8$  white Teflon matrix as shown in figure 23. This matrix is highly reflective in the visible range (reflectivity  $R = 98,3 \%$ ). It reduces the crosstalk between the channels and prevents photons from scattering from one channel to the other. In addition a silicone pad is placed between each crystal and APD for better optical and mechanical coupling. The quantum efficiency of the APD is about 0.75 electrons per incident photon.

The scintillator material is LSO ( $\rightarrow$ sec.2.4.1, p.9)). Figures 23 - 30 show the most important parts of the detector modules.

#### 4. PET System and Components

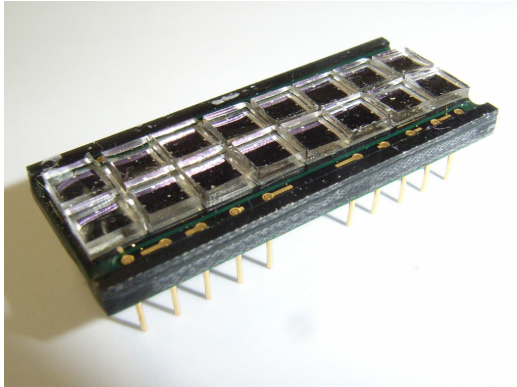


**Figure 23:** APDs arranged in a  $2 \times 8$  matrix with silicone pads on top. At the side of the board, the feedthroughs of the pins lie open.

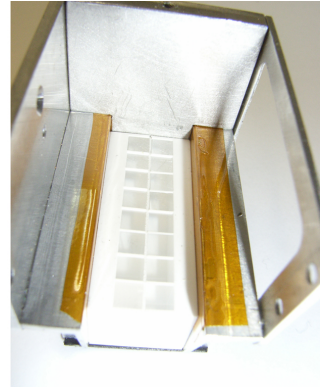


**Figure 24:** LSO crystals assembled in the white PTFE matrix.

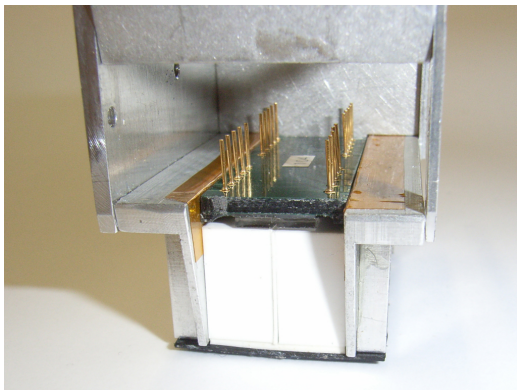


**Figure 25:** Open side view of detector head with APDs on top of the crystals.



**Figure 26:** Connection of the APDs to the detector module and the preamplifiers.

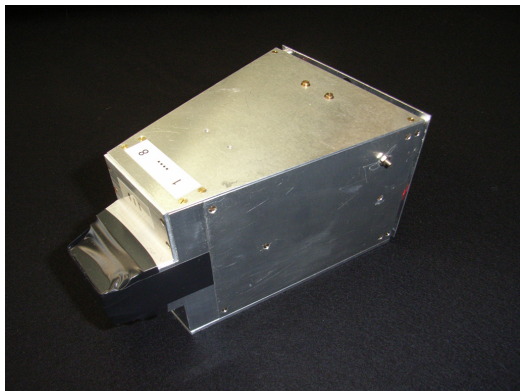


**Figure 27:** Complete detector module. The APDs with the LSO crystals are under the black taped detector head.

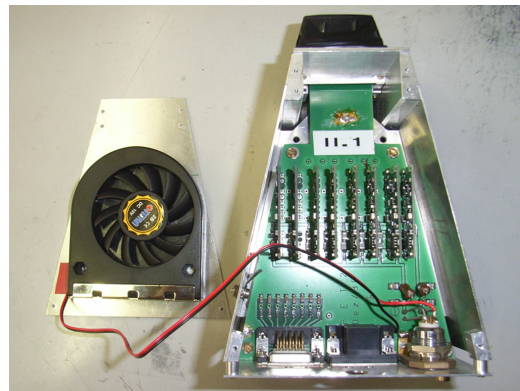


**Figure 28:** View of the preamplifiers, one for each channel. All modules are air-cooled from top and bottom.

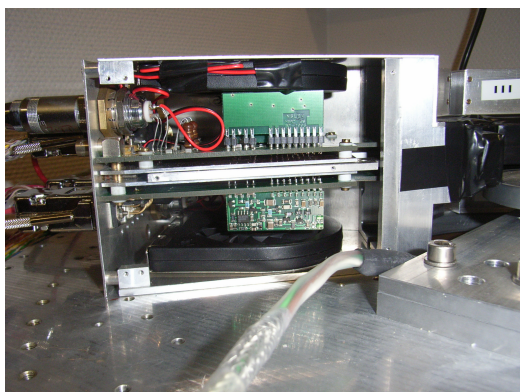


**Figure 29:** Side view of a detector module with removed housing.

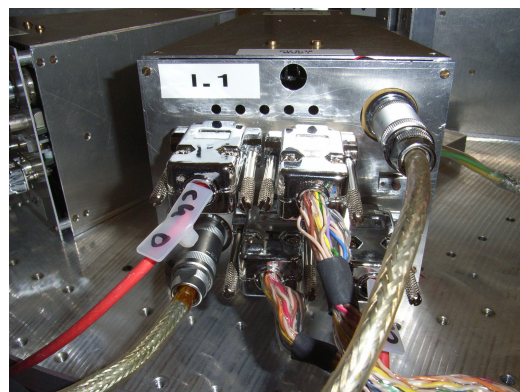


**Figure 30:** Rear view of a detector module with the connectors for upper and lower row. The red wire supplies high voltage, the varicoloured cable feeds the signals out and the silver cable supplies  $\pm 12$  V.

## 4.2. Radioactive Sources



**Figure 31:** Top view of the plexiglas source with TUM logo inside. The logo gets filled with activity, the cap can be taken off. The two screws in the middle of the cap are for filling and de-aeration.



**Figure 32:** View of a source with removed cap. The o-ring between cap and base seals the source.

For the image reconstruction during the lab course, four sources with different symbols milled in are available. The milling is exactly as deep as the height of the LSO crystals in the detectors and is supposed to get filled with radioactivity. So the symbols should get visible again in the reconstructed image.

## 4.3. Electronics and Software

### 4.4. SADC Basics

#### Signal Sampling

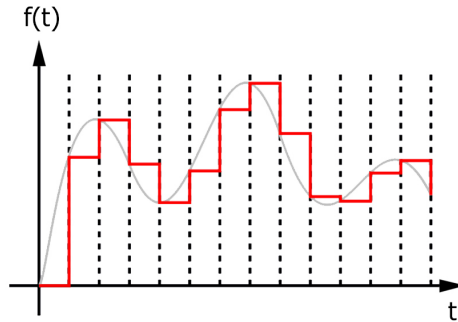


**Figure 33:** Illustration of signal sampling. The analog pulse (grey) is converted to digital values in equidistant time intervals (red).

In general, an *Analog to Digital Converter* or short *ADC* converts continuous analog electric signals into discrete digital numbers both in amplitude and time. This is called signal sampling. The main parameters of the ADC are its resolution and its sampling frequency. The ADC for the lab course has a resolution of 10 bit and  $f_s = 80$  MHz which results in a distance of  $T_s = \frac{1}{f_s} = 12.5$  ns per sampling point. Each sampling point carries a time stamp and owns information about the pulse-height. For example, let  $f(t)$  be a continuous signal that is sampled, with  $t$  the time. The samples are taken equidistant in time; thus the digitized signal gets staircase-shaped ( $\rightarrow$ fig.33). A fundamental statement for sampling is the Nyquist-Shannon sampling theorem. It states, that if the function  $f(t)$  contains no frequencies higher than  $X$  hertz, it can be completely reconstructed with a sampling rate higher than  $2 \cdot X$ . This is the case for our signals as they are rather slow and the time between rise and fall is several tens of ns.

#### Time Information

To extract the time information from an analogous signal pulse, one of the most common methods called constant-fraction timing. Figure 34 shows the principle. First, the input signal is split into two parts. One part is attenuated to a fraction  $f$  of the original amplitude, the other part is delayed and inverted. Both signals now are added to form the constant-fraction timing signal. As a result, the sum of both signals yields a bipolar signal with a zero-crossing, which corresponds to the original point of optimum fraction on the delayed signal. Now, a discriminator can trigger on the zero-crossing and provide a time stamp at the optimum fraction of the pulse height. The time of zero-crossing is independent of the pulse amplitude and is therefore very precise. This discriminator is called constant-fraction discriminator or

#### 4. PET System and Components

short CFD [KNO]. Our SADC uses a more efficient digital implementation for the time determination [MAN].

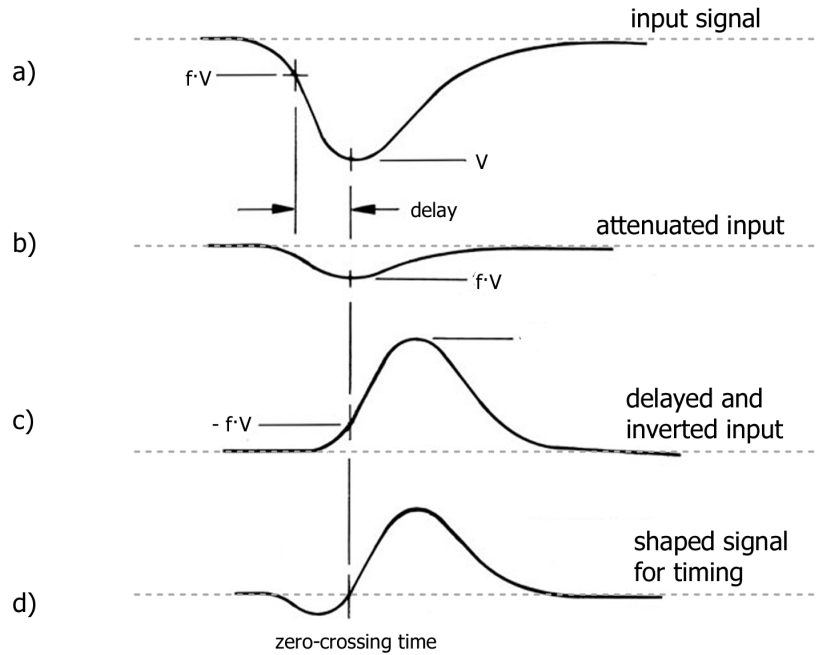


**Figure 34:** Principle of constant-fraction timing.

#### 4.5. Linux

Linux nowadays is established as an operating system and is widely used in science and research. It is a standard tool for modern physicists. This lab course offers and encourages to learn and use basic features and get in touch with Linux. Its benefits are the free availability without additional costs as well as many programs often coequal to commercial ones.

The used Linux distribution for this project is Ubuntu 8.04 LTS [UBU], chosen due to its support up to April 2011, stability, user friendliness, easy serviceability and upgrade capability. It features the GNOME window manager.

A short introduction to the most basic commands needed for the lab course can be found in app.C, p.46.

#### 4.6. ROOT

The software used for the data analysis is ROOT. It is an object oriented framework written in C++. It is developed and maintained by CERN starting in 1994 by René Brun and Fons Rademakers to handle the high amount of data produced by high energy physics experiments. Relevant for the lab course are these features:

- Histogramming and displaying of distributions and functions.
- Fit tools.
- Standard mathematical functions.
- Tree objects for storing data.
- Accessibility of ROOT's C++ classes by external programs.

ROOT comes with a C++ command line interpreter (CINT), by which the classes of ROOT can be accessed. It is freely available for Linux, Windows, MAC OS X and Solaris. [ROO]

## 5. PET System Commissioning for the Lab Course

**Note:** This section shows step by step, how to commission the PET scanner. It is necessary for the lab course. Since all steps either have to be done directly at the scanner or the readout PC, do not be worried if you do not completely understand all steps during your preparations. This section is a guideline to operate the PET system and enables you to solve the tasks during the lab course (→sec.6, p.40).

### 5.1. High Voltage Rampup

Since the control software for the high voltage module only runs under Windows, *VirtualBox* has to get started by either selecting it from the *Applications* menu or press *Alt+F2* and enter *VirtualBox*. VirtualBox is a virtualization software for running different operating systems on a host system. After it has started, a window will show up with an icon for Windows XP in its left panel. Double click it, Windows will start up in a new window. If bootup is finished, the *isegCANHVControl* program can be started via the icon on the desktop. There are two modules listed (EHS 62 and EHS 63), their channels can be controlled by clicking on a module (→fig.35). EHS 62 controls ch0-7 and EHS 63 is for ch8-11. In the main window, different profiles can be loaded via *File* → *Open a profile*. The profile *isegHV\_allch\_200V\_ON.prf* ramps up ch0-11 to 200V, *PET\_isegHV\_allch\_ON.prf* switches all channels on with the correct voltage settings for the detector system and *PET\_isegHV\_allch\_OFF.prf* switches all channels off. The channels can be monitored via the channel control window, which opens by clicking on a module (→fig.36). Settings for a specific channel can be set by right-clicking on it.

To protect the APDs from damage by improper handling, the hardware limit is set to 410 V and the hardware current limit is set to 0.6 mA. The ramp speed is 5 V/s, so the rampup procedure takes about 80 seconds.



**Figure 35:** Main window of isegCANHV-Control running under Windows XP using VirtualBox.



**Figure 36:** Channel control window of isegCANHVControl.

## 5.2. SADC Configuration

For loading the SADCs, the upper left green LED on all SADCs and both red LEDs on all J2-USB cards have to be on. Otherwise the implemented firmware of the SADCs or the J2-USB cards was not loaded correctly. If so, a power cycle is necessary. A description of the different LED states can be found in figures 37 and 38.

### Initialization

The firmware of the FPGAs (Field Programmable Gate Array) on the SADCs has to be loaded via the PC, which enables the SADCs to take data. In the terminal, change directory to `/home/pet/SADC/sadconfig/` and type

```
./load_all_adcs.sh
```

to load all SADCs one after the other. The red firmware LED on the USB card shows that the configuration is ongoing (→fig.38). Once it is finished, all green LEDs on the SADC are on and show the successful loading of the two FPGAs.



**Figure 37:** LEDs at the SADCs, in loaded state.

*SADC powered:* upper left green LED on.

*SADC loaded:* all green LEDs on.

*Incoming data:* lower left orange LED blinking.

*Overflow or clock lost:* lower middle red LED blinking or on.

*Firmware error:* lower right red LED on.

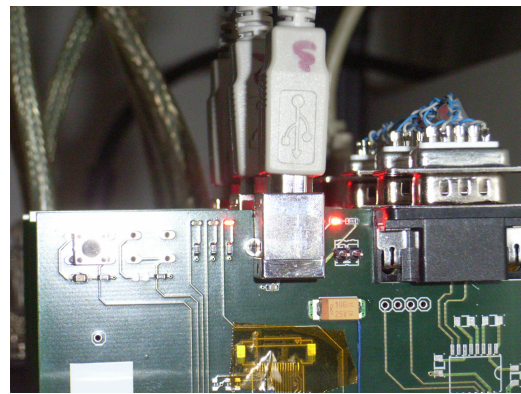


**Figure 38:** Red LEDs to the left and right of the USB connector at a J2-USB card.

*Firmware loaded:* left LED on.

*USB connected:* right LED on.

### Configuration

Up to now, the FPGA firmware is configured with standard values not necessarily correct for our readout system. To change these register settings,

## 5. PET System Commissioning for the Lab Course

go to `/home/pet/SADC/regconfig/`.

For loading the predetermined correct register settings of all SADCs, use the script

```
./setreg_allADC_FDG.sh
```

This will now automatically configure the registers for a readout with FDG or  $^{22}\text{Na}$ .

### 5.3. Taking Data

#### Data readout for detector calibration

For the calibration of the modules and to have a first look at the spectra of FDG or  $^{22}\text{Na}$ , it is not necessary to rotate the source. To read data from the SADC modules at a fixed projection angle, the program `sadccdata` from `/home/pet/SADC/sadccdata/` is used. It reads the data blockwise from the USB cards and formats the output according to the command line options.

For a test, if data is coming from all three SADCs, type

```
./sadccdata -A
```

This does not write anything to a file, but the datarates coming from each SADC are displayed. Without any source placed inside the scanner, typical datarates for each SADC are 20 to 30 kB/s. With an activity of 1 MBq, the datarates are about 200 to 500 kB/s for each SADC.

To read the data from all SADCs and write it to a file, use

```
./sadccdata -A -f <datafile.dat> -t <time[seconds]>
```

where `<datafile.dat>` specifies the output file and `<time[seconds]>` how long data will be taken. This file is the basis for the later data analysis. It is strongly recommended to place the files in directories with the format `[year]-[month]-[day]-[source]`, name the files `data<X>.dat` and number them consecutively, specified with `<X>`.

*Note:* the directory has to be created before.

Example: `/home/pet/DATA/2009-06-22-Na22/data1.dat`

The blinking of the orange LEDs at the SADCs signalize data taking, an additional blinking of a red LED means that there is an overflow in data. Usually this is a hint that either the high voltage settings or the threshold register settings are not correct, resulting in too high data rates from the detectors.

To have a look at the recorded spectrum in real-time, use

```
./sadccdata -d4 -A | ../streamusb/streamusbhist [ch] > /dev/null
```

where `-d4` formats the output to 32 bit words (4 · 8 bit). The pipe `|` streams the output of `sadccdata` to `streamusbhist`. The channel to investigate is set with `[ch]`. For performance reasons, `>` dumps the screen output of `streamusbhist` to `/dev/null`. The program `streamusbhist` will build up a spectrum as soon as data comes in, the

program can be canceled using `Ctrl+C` in the terminal.

Having a look at the spectra while data taking is very useful to get a fast overview and helps setting the high voltage and the right thresholds for each channel.

## 5.4. Create ROOT Tree

For storing data, ROOT uses a format called 'tree'. These tree-files are created from the raw data files with a C++ program. A tree itself can be seen as a trunk with different branches with leaves which can be filled with data. The leaf is the data container while grouping is the branch's job. For example, the data of our PET scanner is sorted into the tree with one branch for 'events' and another one for 'data'. The first contains leaves with the recorded events like peak maxima or signal baseline for the channels, and the latter contains the ADC pulse samples, which are currently disabled while taking data for performance reasons.

Creation of the tree is done by the program `createtree`, which can be found on the readout PC at `/home/pet/analysis_software/createtree`. The usage is

```
./createtree tree-data-<X>.root -b data<X>.dat
```

which creates as output the tree specified with `tree-data-<X>.root` by reading the raw data from `data<X>.dat`. `<X>` is the number of the file. The option `-b` is necessary to tell `createtree`, that the datafile is in binary format, which is the case if the option `-d4` has not been given to `sadcdata`.

Example: `./createtree tree-data1.root -b data1.dat`

The following data analysis, detector calibration as well as the image reconstruction all are based on the ROOT tree.

## 5.5. Energy calibration

### General Remarks

The gain of APD detectors and the light output of LSO scintillators are both very sensitive to temperature changes. Thus, for a given incident photon energy, the amplitude of the measured signal is varying. In addition, APDs differ slightly in their signal properties like e.g rise time and required trigger threshold. Different signal delays for each APD may be caused by different cable lengths. So a constant ambient temperature and stable environment conditions are necessary during the operation. Calibration before every measurement is a must.

### Introduction

The energy calibration assigns the physical energy value of the detected photon to the digital value of the signal pulseheight.

Figure 39 shows a typical energy spectrum of a single channel. The incoming signal pulseheight corresponds directly to the detected energy. A higher energy deposit in the detector correlates to higher ADC channels. Here the signal peak maxima are

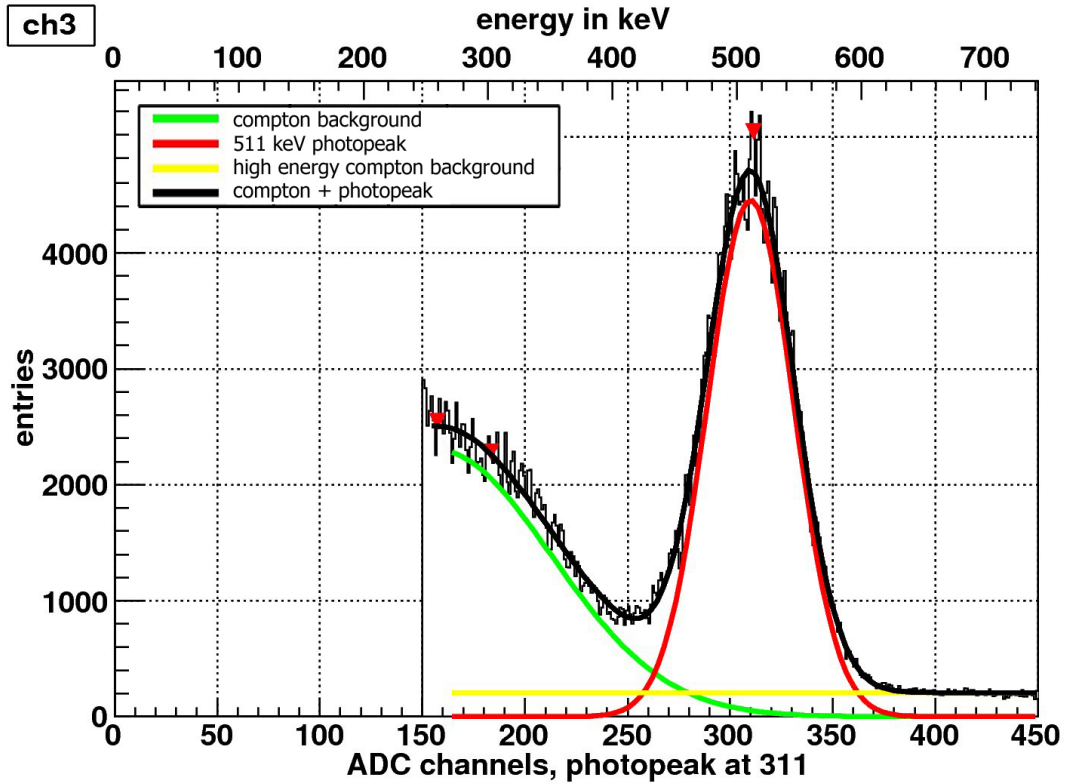


**Figure 39:** Energy spectrum of one APD from a  $^{22}\text{Na}$  source with calibration. The black line is the sum of the different regions in the spectrum (red, yellow, green). Their reason should be explained in the evaluation.

histogrammed, which means that every hit of a certain ADC channel adds one entry to the histogram. Their sum leads to the characteristic energy spectrum with the photopeak at 511 keV. The calculated energy axis is on top of the histogram, based on the mean value  $\mu_p$  of the gaussian fit to the photopeak. The calculation of the energy  $E_c$  for a given ADC channel  $c$  is done by:

$$E_c = 511 \text{ keV} / \mu_p \cdot c_{\text{ADC}} \quad (13)$$

Here, a cut of the data has been made at ADC channel 150 to reject unnecessary events, e.g. compton scattered photons and the characteristic noise of the APD. The APD is operated in avalanche mode just short below its breakdown voltage. In this operation mode, room temperature is sufficient to get small signals due to breakdowns. The low energy cut has to be set individually for each channel by choosing an appropriate threshold, which is done via the SADC register settings ( $\rightarrow$ sec.5.2, p.29).

### Energy Spectrum

Starting from the ROOT tree file created in sec.5.4, the energy spectra of each APD

can be investigated. ROOT can be started by opening a terminal and entering `root`. A splash screen appears and CINT, the ROOT command line C++ interpreter, is displayed (→fig.40). Here basically every C++ statement can be given as input and directly interpreted.

Entering `new TBrowser` to starts the graphical user interface. The *ROOT Object Browser* window will pop up (→fig.41). To open a file, browse to its path in the left panel and double click it. It is now opened and accessible at *ROOT files* in the left bottom panel of the browser window, double click displays its contents. To investigate the tree, right click it in the right panel and select *StartViewer*, which starts the *Tree Viewer* displaying all branches and leaves (→fig.42). To draw a histogram

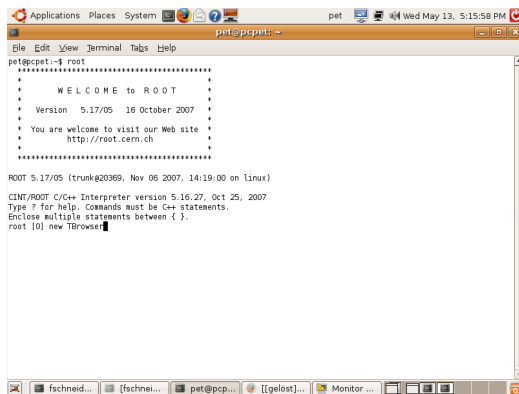


Figure 40: ROOT console window.

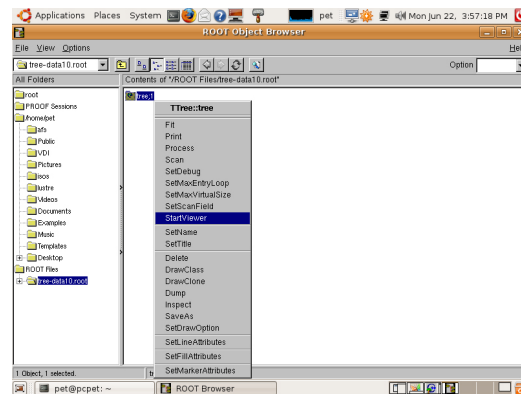


Figure 41: ROOT Object Browser.

of a certain leaf, just double click on it. The leaf *event.maximum* contains the peak maxima for all channels, a doubleclick draws a histogram which is smeared as all channels are drawn at the same time. To create a cut on a single channel, an empty *expression* is used. Double click an empty expression, and the *Expression Editor* will pop up. The first line states the condition and accepts C++ statements as input, e.g. for selecting only channel 0, type `event.channel == 0` (logical equality in C++ uses `==`, a single `=` is an allocation). *Alias* is the description of the expression, put here e.g. `ch0`. Up to now, the scissor symbol is empty. To apply a cut, drag and drop the just created expression `ch0` to the scissor symbol and let it catch. Now the cut is active for all data sets that have been dragged either to the *X: Y:* or *Z:* statements above the scissor. Double click on the scissor either enables or disables the cut. As we want to draw an energy spectrum for a single channel, drag the leaf with *event.maximum* to the *X:* statement and let it catch. The histogram is drawn by clicking on the *Draw current selection* button in the lower left of the window. It should look similar to the one shown in figure 43.

To load expressions which contain cuts for all 96 detector channels to the *Tree Viewer*, click *File Open Open session ...* and browse to `/home/pet/DATA/MADPET-cuts-96ch.C`.

## Fitting and Energy Resolution

To calculate the energy resolution of a detector channel, a gaussian function must

## 5. PET System Commissioning for the Lab Course

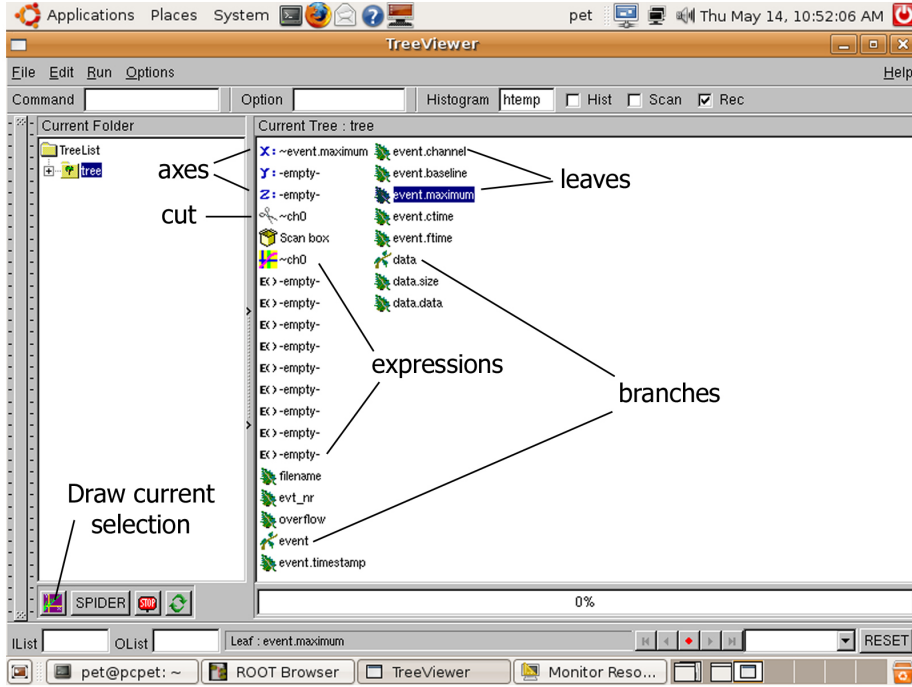


**Figure 42:** Tree Viewer

be fitted to the photopeak. In the histogram window ( $\rightarrow$ fig.43), right click on a horizontal part of the drawn entries and select *FitPanel*. Choose the predefined *gaus* as fit function and set the range with the slider at the bottom of the window to the region of the photopeak. Then click *Fit*, the gaussian will show up. The fit parameters can be displayed directly in the histogram by selecting *Options* $\rightarrow$ *Fit Parameters* in the menu bar of the histogram window.

From the fit and its parameters, one can extract the relative energy resolution defined as

$$\frac{\Delta E}{E} [\%] = \frac{\sigma_f}{\mu_f} \cdot 100 \quad (14)$$

with  $\sigma_f$  the standard deviation and  $\mu_f$  the mean of the fit. The smaller  $\frac{\Delta E}{E}$  the better the energy resolution, as the peak gets more narrow. One can state  $\sigma_f$  also in terms of energy. This is possible, as an ADC signal of amplitude 0 corresponds to no energy deposit in the detector.

$$\sigma_{\text{energy}} [\text{keV}] = \sigma_f \cdot \frac{511}{\mu_f} \quad (15)$$

The FWHM (full width at half maximum) can be calculated by

$$\text{FWHM} [\text{keV}] = 2\sqrt{2 \ln 2} \cdot \sigma_{\text{energy}} \approx 2.35 \cdot \sigma_{\text{energy}} \quad (16)$$

To quit ROOT, either close its terminal window or enter `.q` at the command line.

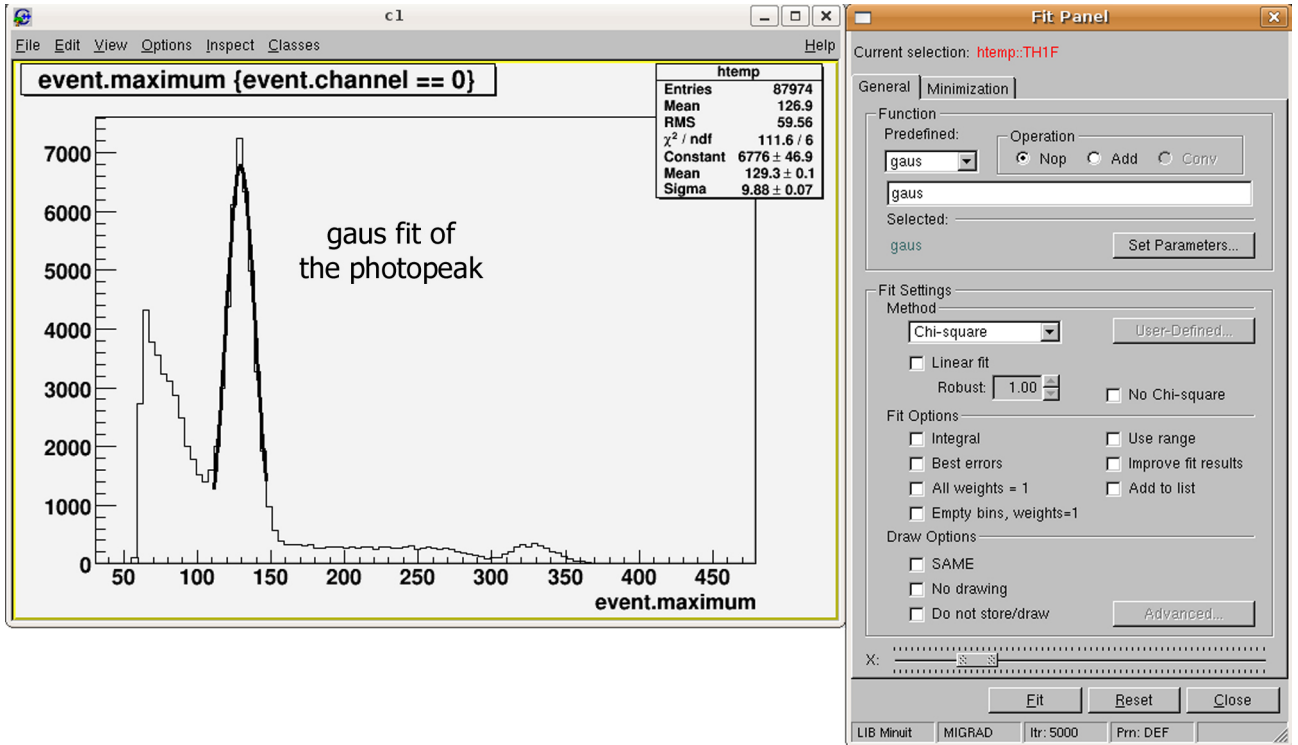


**Figure 43:** Gaus fit of the photopeak. The fit parameters can be displayed in the histogram and used to determine the energy resolution. Here:  $\sigma_f = 9.88$ ,  $\mu_f = 129.3$

### Automated Software Procedure

The energy calibration procedure cannot be done manually for all 96 channels in a reasonable time. This why you will do the manual procedure exemplary just for one channel. All other channels will be calibrated automatically and the resulting histograms are merged into one *\*.pdf* file.

For this, the script at `/home/pet/analysis_software/ehist_all` is used:

```
./ehist_all.sh <input.root> <outputdirectory> reads the data from the
<input.root> tree file and writes ecalib.root and allch.pdf to <outputdirectory>.
ecalib.root is used e.g. as input for the image reconstruction and the timing
calibration program tcal, described in the following section. All channel his-
tograms are written to the file allch.pdf. This gives a better overview of all
channels and makes a check of the calibration correctness easier.
```

## 5.6. Time Calibration

### Introduction

Essential for PET and the image reconstruction is the exact time of detection for each registered photon. Mismatched timing leads to a loss of LORs and takes more random events (or short randoms) into account, since the coincidence window has to be chosen larger. The time calibration has to correct the time delays between the

## 5. PET System Commissioning for the Lab Course

channels, which are e.g. caused by unmatched cable lengths or different preamplifier properties that may change the signal timing.

During the search for LORs ( $\rightarrow$ fig.44) between the detectors, the time stamps of all LOR events from one channel are subtracted from all time stamps of the opposing 48 channels. This leads to a time difference histogram, adding one binary for each calculated time difference. Ideally this should give a sharp peak around zero, but in reality there is a distribution that can be fitted by a gaussian ( $\rightarrow$ fig.45). The reason is the limited time resolution of the detector and the electronics. It can be determined similar to the energy resolution with the help of the standard deviation  $\sigma$  and the mean  $\mu$  of a gaussian fit function ( $\rightarrow$ sec.5.5).

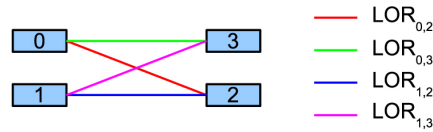


**Figure 44:** Example with 2 versus 2 detectors in coincidence and the possible LORs. [MAN]

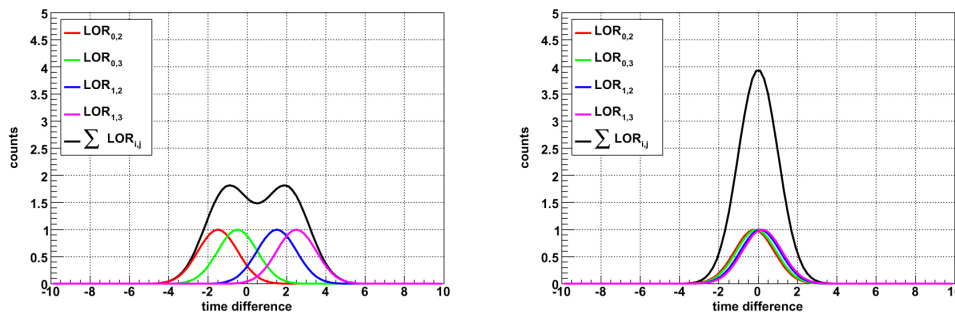


**Figure 45:** Timing histogram for the different LORs.

*Left, uncalibrated:* Unmatched timing leads to a large time difference and a broadening of the gaussian distribution, requiring a wider coincidence window.

*Right, calibrated:* Correct timing squeezes the gaussian for better time resolution allowing a more narrow coincidence window. [MAN]

The more narrow one can choose the coincidence window, the better gets the signal to noise ratio of the image. The window size defines what range around the zero value of the timing histogram is accepted as valid coincidence and used for image reconstruction. Events outside the coincidence window are discarded.

### Time Resolution and LORs

For understanding the principle and necessity of the time calibration, you are asked to determine the time resolution of the system before and after calibration. This shows the impact on the width of the coincidence window.

Again, the created ROOT tree provides the input data. The program `tcal` can be found at `/home/pet/analysis_software`. The usage is

```
./tcal [tcalib.root] [ecalib.root] low_thr[keV] high_thr[keV] [output.root]
[input.root]
```

where

`[tcalib.root]` is the input file that has been created during the previous time calibration. As this file is not available when running `tcal` the first time or before the automated calibration has been done, state 1 as argument.

`[ecalib.root]` is created by the energy calibration program. If it is not available, state 1 instead.

`low_thr[keV]` sets the lower threshold of the energy cut in keV. Data samples of energies below are thrown away. Empirically, a value of 480 has been proven of value not to loose any 'good' data but to reject Compton scattered events.

`high_thr[keV]` sets the upper limit for the energy that is taken into account. Here a value of 700 is usually set.

`[output.root]` specifies the output file where `tcal` saves its results.

`[input.root]` are the ROOT tree files that have been created from raw data. Multiple files as input are possible. E.g. stating `tree*.root` takes all ROOT tree files in the specified directory as input.

To investigate the output file, open it in ROOT using the TBrowser:

`global_p` is the timing histogram. It shows the different delays of the found LORs. `tcal` already fits a gaussian to the peak and shows FWHM and the  $\sigma$  of the fit. According to the value of FWHM, the coincidence window is set.

### Data readout for image reconstruction

The image reconstruction requires data from different projection angles, since we use a sectorized tomograph. The approach is to take data for a given time, then rotate the stepping motor to the next projection and take again data - until one revolution of the source is complete. For each projection angle, a single data file is produced and consecutively numbered. The measurement time is the same for all projections. This procedure is done by the script `takedata-all.sh` located at `/home/pet/SADC/sadcddata/`. Its usage is

```
./takedata-all.sh <time[seconds]> <stepwidth[degree]> <outputdirectory>
```

## 5. PET System Commissioning for the Lab Course

which takes data and afterwards does all the necessary calibration for the image reconstruction. It creates a ROOT tree file from every datafile, a pdf file with spectra of all channels, the energy calibration file `<outputdirectory>/ehist/ecalib.root` and the calibrated timing histogram `<outputdirectory>/tcal/tcalib.root`.

*Note:* `<outputdirectory>` must be stated as absolute path.

Example:

```
./takedata-all.sh 60 45 /home/pet/DATA/2009-07-31-FDG-45deg-60sec-1MBq
```

## 5.7. Image Reconstruction

### Prerequisites and Procedure

The before acquired ROOT tree files are the basis for the sinogram. It is created

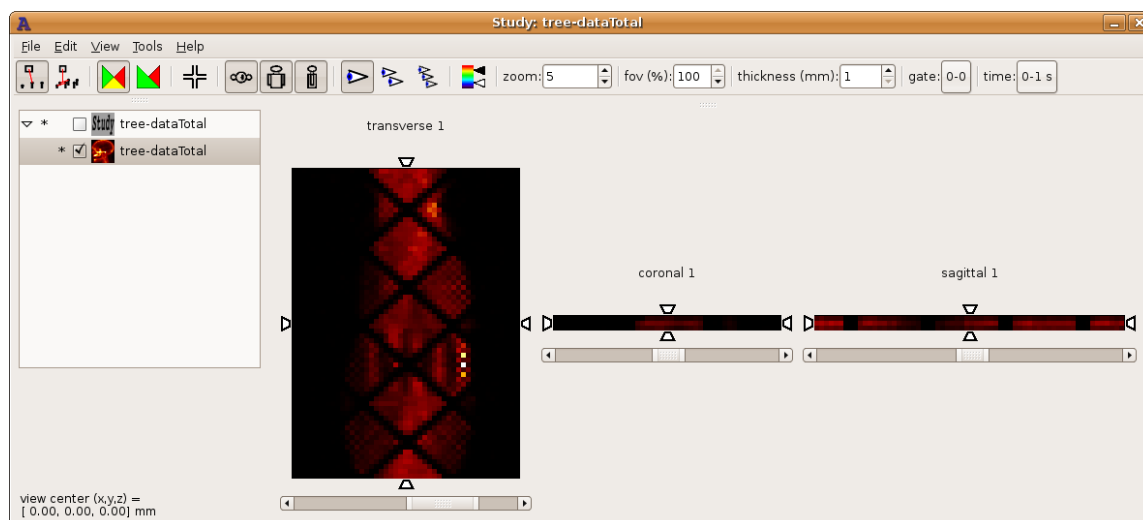


**Figure 46:** Screenshot of amide with a sinogram of the TUM source. The large black lines crossing the sinogram arise from the spacing between the detector modules.

with the script `buildsinogram.sh` located at `/home/pet/SADC/sadcddata`:

```
./buildsinogram.sh <stepwidth[degrees]> <inputdirectory>
```

The rotation step width in degrees must be set and the files in `<inputdirectory>` will be processed. The output goes to `<inputdirectory>/reconstruction`, where the BP and FBP results are saved as `*.ahv` files. When finished, amide will open showing the sinogram (the file `tree-dataTotal.hs` in `<inputdirectory>`) and the results of BP and FBP. Amide is a free tool for viewing, analyzing and registering volumetric medical imaging data sets [AMI].

*Note:* `<inputdirectory>` must be stated as absolute path.

Example:

```
./buildsinogram.sh 45 /home/pet/DATA/2009-07-31-FDG-45deg-60sec-1MBq
```

To get rid of the randoms in the final sinogram, a random estimation is done. The procedure is to have a look at a larger and delayed time window with a width of 6 times the coincidence time window. It starts after finding a valid LOR with a delay of 5 times the coincidence window. One assumes, that all events registered in the delayed time window correspond to randoms, which are subtracted from the final sinogram. This method of course is only an estimation, the set time values for the delayed window are empirical.

## 6. Tasks

### 6.1. General Remarks

The questions or statements written in italic shape must be answered and presented in the evaluation.

### 6.2. Power Up and Configuration

#### 6.2.1. Investigating the signal

First, check all cables and power the system by switching on the power crate and the readout PC. A radioactive source may not be used yet.

Before loading the SADCs, unplug the flat data cable at the SADC of Module VI and plug it into the Lemo fan-out next to the scanner. Each Lemo connector represents one channel. Connect a Lemo cable to the oscilloscope and inspect the signals. At the scope, switch the bandwidth limit on. Now, ramp up the high voltage to 300 V, as described in sec.5.1, p.28 (EHS 63, ch2 in the `isegCANHVControl` software corresponds to Module VI.1).

Do not only check one channel, but also the other 7 ones. Ramp up the voltage further, e.g. in 10 V steps. *At which voltage does the first APD of Module VI.1 start to deliver a signal? At which voltage does the first of the APDs have its breakdown? Which one?* Do not exceed 410 V!

The final operating voltage should be at least 4 V below the breakdown voltage. Check again all other 7 channels of Module VI.1 with the scope. No APD may break down for the scanner operation.

After the voltage adjustment, let your advisor place and remove the  $^{22}\text{Na}$  source in front of the detector.

*Why is the signal negative? What is the pulseheight and risetime? How does the signal behaviour change when applying high voltage to the APDs? How does it change with the radioactive source in front?*

#### 6.2.2. Loading the SADCs and Aquisition of the first Spectra

Replug Module VI to the SADC. Before loading the SADCs, ramp up the high voltage with the correct settings for all channels by loading the appropriate profile in `isegCANHVControl` ( $\rightarrow$ sec.5.1, p.28). When all channels are completely ramped up, load and configure and set the registers of the SADCs. Look at the noise with `sadcdata` and `streamusbhist` ( $\rightarrow$ sec.5.3, p.30).

Now let your advisor place the  $^{22}\text{Na}$  point source inside the scanner's field of view. Again take data with `sadcdata` and have a look at the energy spectra of some channels with `streamusbhist` ( $\rightarrow$ sec.5.3, p.30).

## 6.3. Calibration

### 6.3.1. Energy Resolution

Start taking data for 3 minutes and write it to a file with the help of `sadccdata`. Afterwards, let the advisor remove the  $^{22}\text{Na}$  source due to radiation protection, as it is no longer needed for the data analysis at the readout PC.

Out of the datafile, create a ROOT tree using `createtree`, afterwards start ROOT and open the tree file. Select one channel, plot it and fit a gaussian to the photopeak (→sec.5.5, p.31).

*Explain the different regions and peaks in the spectrum. What is their cause?*

*What is the energy resolution for this channel? Calculation? Save an image of your fit.*

Do the automatic calibration procedure with `ehist_all`, which creates as output a pdf file with the calibrated spectra of all channels and the energy calibration file `ecalib.root`. It must be used for the following time calibration and also the image reconstruction. Investigate `ecalib.root` with ROOT.

*What is the meaning of the histogram contained in `ecalib.root`? Attach the pdf file with all channels to your evaluation.*

Now, lower the preset high voltage for a module of your choice) in 0.5 V steps for 6 different voltages. Build the spectra of all channels as described above. Choose some channel of your selected module and check the photopeak position. Write down its value in ADC channels. *How does the position of the photopeak behave due to the voltage change? Select one channel, make a plot and try a fit!*

### 6.3.2. Time Calibration

Starting from the ROOT tree, create the coincidence timing histogram `global_p` for the uncalibrated case (→sec.5.6, p.35). *Save the plot for your evaluation as \*.png file.* Now calibrate the scanner with 3 iterations.

*Again save your results as \*.png files. What is the FWHM difference for the calibrated and uncalibrated case? Compare your results. What size would you choose the coincidence time window at least?*

*Is it possible to do time of flight measurements of the annihilation photons? Explain.*

## 6.4. Image Reconstruction

Now let your advisor fill one of the plexiglass sources with FDG. Remember the initial activity and the start time of your measurements. Place it into the scanner. Take data with the script `takedata-all.sh` located at `/home/pet/SADC/sadccdata`, which includes the energy and time calibration. As parameters, state the measuring time, the rotation angle and the output directory (→sec.5.7, p.38). The convenient values are either  $45^\circ$  or  $20^\circ$  for the angle and 1 or maximum 2 minutes for the measuring

## 6. Tasks

time per projection.

When finished, use the script `buildsinogram.sh`, which creates the sinogram and applies BP and FBP ( $\rightarrow$ sec.5.7, p.38). In amide, try some color map options, rotate your image and try setting contrasts. *Save your results as \*.jpg image, e.g. do a screenshot of amide or export your view. Comments on the pictures? Differences between BP and FBP? What is the origin of the black lines in the sinogram?*

The FDG is decaying during the measurement. *Can you think of a way, how to extract its half-life from the measured data? (Hints: Use the files measured at the different projection angles. A plot and a fit are also very helpful.)*

Ask the advisor to fill another plexiglass source. Try the completely automated image reconstruction (your advisor knows how to do that). *Save your results for your evaluation. Comments?*

*Estimate the scanner's spatial resolution with the help of the dimensions of either the bubenog or skyscraper source given in app.B, p.45.*

## Appendix

## A. Location of the Lab Course

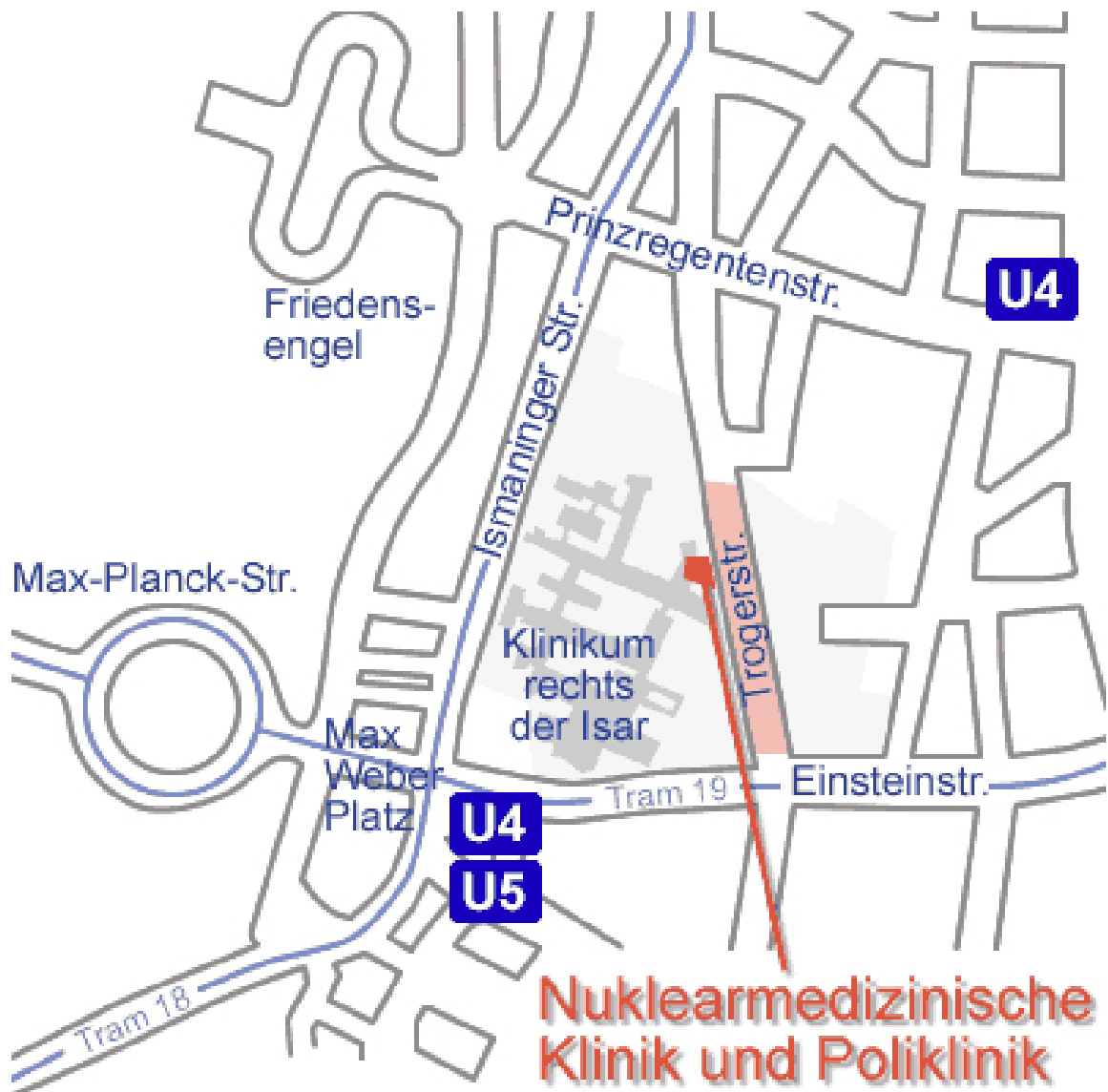
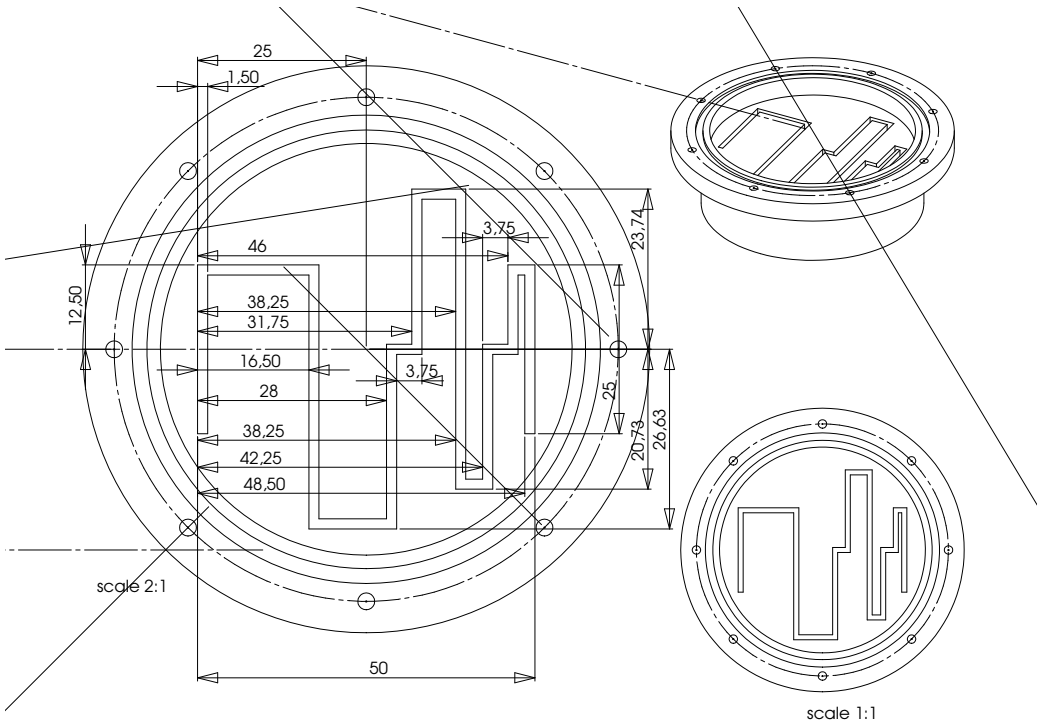
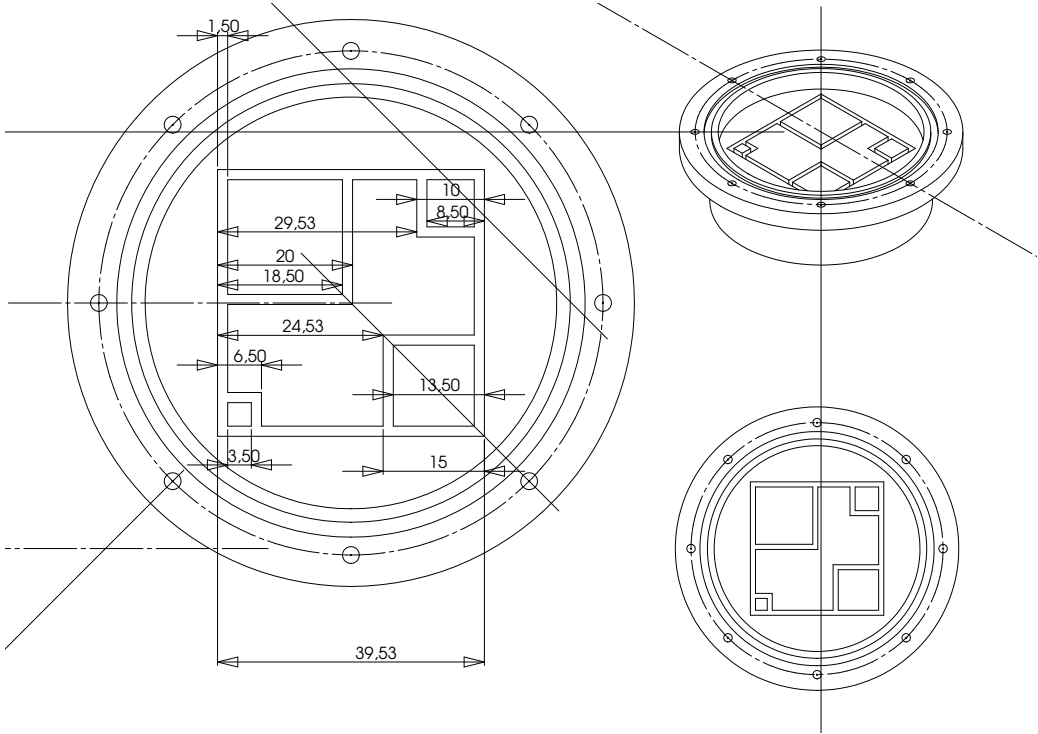


**Figure 47:** Location of the Lab Course at the Klinikum Rechts der Isar.

# B. Dimensions of the Bubenog and Skyscraper Sources



## C. Linux Commands

This lab mainly uses the *terminal* as command line tool; the usage of the graphical user interface (GUI) of Ubuntu is straightforward and should be self-explanatory. With intent, most programs of this lab course run without a graphical user interface (GUI) to get the students closer to programming and beneath the surface, not just to click some buttons. To get prepared, the most used commands that are also needed for the lab are explained here. Note that Linux commands are case sensitive.

To open a terminal, click *Applications* → *Accessories* → *Terminal* in the menu or press *ALT+F2* and enter `gnome-terminal`. The starting directory is the home folder (→fig.48). The first line `pet@pcpet:~$` states the username `pet`, `pcpet` is the name of the workstation one is logged on, `~` means that the current directory is the home directory and `$` ends the line. If one starts typing a command, press the *tab*(⇐)

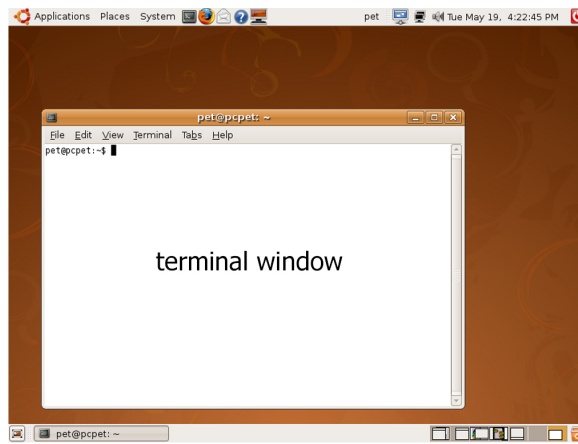


**Figure 48:** Screenshot of Ubuntu with an open terminal window.

key and the system will try to autocomplete or make proposals. For each command, help and options can be displayed by typing `[command] --help`. The most used commands are:

`ls` shows the contents of the current directory. `ls -l` shows the contents as list with details for each element.

`cd` changes the directory up in hierarchy, directories are separated by a slash /  
Example: `cd SADC/sadcddata`

`cd ..` navigates one directory down in hierarchy.

`mkdir [directory]` creates the specified directory.

`rmdir [option] [directory]` removes the specified directory. If it is non-empty, use `--ignore-fail-on-non-empty` as `[option]`.

The terminal saves a history of the last entered commands. To see the last typed ones, use *up*↑ or *down*↓ cursor keys. This feature can save a lots of typing and time.

To run a program, use `./[program] [parameter]`. If needed, specify additional parameters. The prefix `./` specifies, that the following is an executable.

*Example:* `./sadcdata -d4`

To stop a running program at any time, use *Ctrl+C* ( or *Strg+C* on a German keyboard).

`gedit` is a comfortable and easy to use texteditor. To open a file for editing, enter `gedit [filename] &`. The `&` is necessary to leave the terminal accessible while `gedit` (or other programs) is running. To run `gedit` without directly opening a file, press *Alt+F2* and enter `gedit`.

The programs used here in the lab course always show a short description and their usage by executing the program without any parameters (e.g. `./<programname>`)

The sourcecode of the programs written for this lab course (e.g. `sadcdata`) can always be found in the same directory as `*.cc` file. It can be displayed with `gedit`.

Recompilation of a program after changing its sourcecode is done using `make`.

A pipe `|` between two programs is responsible for sending the output of the first one directly to the second one.

*Example:* `./sadcdata -d4 | ../streamusb/streamusbhist 12`

The greater-than-sign `>` states the output destination of a program, the smaller-than-sign `<` is followed by the input for the program.

*Example:* `./sadcdata -A > /dev/null`

dumps the output of `sadcdata` to `/dev/null`

*Example:* `./streamusbhist 45 < data.dat`

gives `data.dat` as input to `streamusbhist`

The terminal is quit with `exit`.

For browsing files graphically, klick *Places* → *Home Folder* or *Applications* → *Accessories* → *Thunar File Manger*. Alternatively use *Alt+F2* and enter `thunar`. Inserted media like USB sticks will be mounted automatically and a shortcut is placed on the desktop.

## References

- [AMI] AMIDE. *A Medical Imaging Data Examiner*. <http://amide.sourceforge.net/>
- [BOE] G. Böning. *Verbesserte statistische Bildrekonstruktion für die hochauflösende PET*. PHD in Physics, Max Planck Institut für Physik München, Nuklearmedizinische Klinik und Poliklinik des Klinikums Rechts der Isar München, 2002.
- [DE4] Demtröder. *Experimentalphysik 4. Kern-, Teilchen- und Astrophysik*. Springer, 1998.
- [KNO] Knoll. *Radiation Detection and Measurement*. John Wiley & Sons, 1979, 1st Edition.
- [KUC] T. Mayer-Kuckuk. *Kernphysik*. B.G.Teubner Stuttgart, 1992.
- [MAN] A. Mann. *PHD thesis in preparation*. Electrical Engineering and Communication Technology, Technische Universität München, 2009. <http://e18.physik.tu-muenchen.de/staff/amann.html>
- [MPI] Max-Planck-Gesellschaft zur Förderung der Wissenschaften e.V., Hofgartenstr. 8, 80539 München. <http://www.mpg.de/>
- [MRI] Nuklearmedizinische Klinik und Poliklinik der TU München, Klinikum Rechts der Isar München, Ismaninger Str. 22, 81675 München. <http://www.nuk.med.tu-muenchen.de/>
- [PHE] M. E. Phelps. *PET - Physics, Instrumentation, and Scanners*. Springer, 2006.
- [PIC] B. Pichler. *Untersuchung der Detektoreigenschaften von Lutetium-Oxyorthosilikat-Szintillationskristallen und Lawinen-Photodioden für die hochauflösende Positronen-Emissions-Tomographie*. Diploma thesis in Electrical Engineering and Communication Technology, Technische Universität München, 1996.
- [ROO] ROOT. *A data analysis framework*. <http://root.cern.ch/>
- [SCH] F. Schneider. *Setup and Commissioning of a Positron Emission Tomograph for a Student's Advanced Laboratory Course*. Master thesis in Engineering Physics, Technische Universität München, 2009.
- [STI] STIR. *Software for Tomographic Image Reconstruction*. <http://stir.sourceforge.net/>

- [TEK] Tektronix, Inc. <http://www.tek.com/>
- [UBU] Ubuntu Linux. <http://www.ubuntu.com/>
- [VIR] Sun xVM VirtualBox. <http://www.virtualbox.org/>
- [WUE] T. Würschig. *Aufbau eines Versuchsplatzes für die Positronen-Emissions-Tomographie*. Diploma thesis in Physics, Technische Universität Dresden, Research Center Dresden-Rossendorf, 2005. <http://panda-wiki.gsi.de/pub/Main/ThomasWuerschig/Diplomarbeit.pdf>